The Role of C/EBP-β LIP in Multidrug Resistance

C. Riganti, J. Kopecka, E. Panada, S. Barak, M. Rubinstein
The Role of C/EBP-? LIP in Multidrug Resistance
JOURNAL OF THE NATIONAL CANCER INSTITUTE (2015) 107

JNCI 14-0100R2

Article

The Role of C/EBP-β LIP in Multidrug Resistance

Chiara Riganti[1], Joanna Kopecka[1], Elisa Panada[1], Sara Barak[2] and Menachem Rubinstein[2].

[1]Department of Oncology, University of Torino, Italy; [2]Department of Molecular Genetics, The Weizmann Institute of Science, Rehovot, 7610001, Israel.

Correspondence to: Dr. Menachem Rubinstein, Department of Molecular Genetics, The Weizmann Institute of Science, Rehovot, 7610001 Israel. Phone: +972 8 934 2313. Fax: +972 8 947 0108.

Email: menachem.rubinstein@weizmann.ac.il

ABBREVIATIONS

ER, endoplasmic reticulum; UPR, unfolded protein response; IRE1α, inositol-requiring kinase 1α; PERK, PKR-like endoplasmic reticulum kinase; ATF6, activating transcription factor 6; eIF2α, eukaryotic initiating factor 2α; CHOP/GADD153, CAAT/enhancer homologous protein/growth arrest/DNA damage inducible 153; C/EBP-β, CAAT/enhancer binding protein-β; TRB3, *tribbles*-related protein 3; MDR, multidrug resistance; ABC, ATP binding cassette; Pgp, P-glycoprotein; MRP, MDR-related protein; BCRP, breast cancer resistance protein; LAP, liver-enriched transcriptional activator protein; LIP, liver-enriched inhibitory protein; ERQC, ER quality control.

ABSTRACT

Background Chemotherapy triggers endoplasmic reticulum (ER) stress, which in turn regulates levels of the active (LAP) and the natural dominant-negative (LIP) forms of the transcription factor C/EBP-β. LAP up-regulates and LIP down-regulates the multidrug resistance (MDR) protein P-glycoprotein (Pgp), but it is not known how critical is their role in establishing MDR.

Methods Viability of parental and in MDR tumor cells treated by chemotherapy and by inducers of ER stress was quantitated by crystal violet staining and measuring absorbance at 540 nm. Expression of various proteins was determined by immunoblotting. mRNA levels were determined by quantitative RT-PCR. LIP and LAP were over-expressed using expression plasmids followed by selection with blasticidin. Tumor cells expressing doxycycline-inducible LIP were orthotopically implanted in mice (n=15 mice group) and tumor size was measured daily by caliper. Tumor sections were stained with hematoxylin-eosin and immunostained for Pgp, proliferation and ER stress markers**.**

Results MDR cells do not express basal, chemotherapy-triggered or ER stress-triggered LIP, and fail to activate the CHOP-caspase-3 death-triggering axis upon ER stress or chemotherapy challenge. Over-expression of LIP reversed the MDR phenotype in vitro and in tumors implanted in mice. LIP level was 5-fold lower in MDR cells, probably due to its ubiquitination, which was 3.5-fold higher, resulting in increased lysosomal and proteasomal degradation.

Conclusions Spontaneous and drug-selected MDR cells lack LIP, which is eliminated by ubiquitin-mediated degradation. Loss of LIP drives MDR not only by increasing Pgp expression but also by a twofold attenuation of ER stress-triggered cell death.

INTRODUCTION

Rapidly growing solid tumors are characterized by lagging angiogenesis, leading to hypoxia, nutrient deprivation and accumulation of toxic metabolites. These pathophysiological conditions trigger endoplasmic reticulum (ER) stress (1). The ability of tumor cells to resist stress is a hallmark of aggressive cancers (2, 3). The cellular response to ER stress is termed the unfolded protein response (UPR). During early UPR, cells adapt to stress (1). If ER stress persists, pro-apoptotic proteins such as CHOP (GADD153) and TRB3 are induced (4). Despite different modes of action, many chemotherapeutic drugs – e.g. anthracyclines (5), cisplatin (6), oxaliplatin (5), 5-fluorouracil (7), paclitaxel (8) – share the ability to trigger ER stress (9). Interestingly, chemotherapy efficacy is associated with increased ER stress (10, 11). Hence, activation of the ER-dependent cell death machinery mediates part of the anti-proliferative activity of numerous chemotherapeutic agents.

The frequently observed constitutive or drug-induced multidrug resistance (MDR) is often established by over-expression of integral membrane ATP binding cassette (ABC) drug efflux transporters, such as P-glycoprotein (Pgp/ABCB1), MDR-related proteins 1-9 (MRP/ABCC1-9) and breast cancer resistance protein (BCRP/ABCG2) (12, 13). Pathophysiological conditions promoting ER stress (14, 15) induce the expression of Pgp by unknown mechanisms (15, 16).

The transcription factor C/EBP-β, a crucial activator of the pro-apoptotic CHOP axis (4), is produced in three isoforms, translated from the same mRNA: the liver-enriched transcriptional activator proteins LAP and LAP*, and the natural dominant negative, truncated transcriptional repressor liver-enriched inhibitory protein LIP (17). We recently found that LAP promotes tumor progression by attenuating ER stress-triggered cell death,

whereas LIP exerted opposite effects (18). Of note, LAP activates the transcription of Pgp, whereas LIP inhibits its expression (19).

The aim of this study was to investigate the possible linkage between MDR and ER stress and the role of ER stress-triggered induction of C/EBP-β LIP and LAP in MDR, in chemosensitive and chemoresistant cancer cells of different histological origin and species.

METHODS

Cell Lines

HT29/MDR and A549/MDR cells were generated from parental cells as described (20). Human HT29, A549, JC (21) and Caco-2 (22) cells were from ATCC (Rockville, MD). Please see the **Supplementary Methods** for more details.

Cell Viability and Growth

Counting of viable cells was performed in quadruplicates and repeated four times as reported (18). Please see the **Supplementary Methods** for more details.

In Vivo Tumor Growth

1 x 10^5 JC TetON LIP cells in 20 µl culture medium mixed with 20 µl Cultrex BME (Trevigen, Gaithersburg, MD) were orthotopically implanted according to (23) in 6-week-old female BALB/c mice (15/group). The Institutional Animal Care and Use Committee of the Weizmann Institute of Science approved all animal protocols. Please see the **Supplementary Methods** for more details.

Statistical Analysis

All data in the text and figures are provided as means±SD. The results were analyzed by two-sided analysis of variance (ANOVA). A *P* value of less than 0.05 was considered statistically significant.

RESULTS

The Role of MDR in Resistant to ER Stress

We analyzed the response to chemotherapeutic agents and ER stress inducers in the human chemosensitive HT29 and A549 cells, in the chemoresistant counterpart (HT29/MDR and A549/MDR cells), in the constitutively chemoresistant murine JC cells and in human Caco-2 cells**.** HT29 cells basally express Pgp, MRP1, MRP2 and MRP3; A549 cells basally express MRP1, in line with the pattern of ABC transporters physiologically present in colon and lung mucosa (13). HT29/MDR and A549/MDR cells express higher levels of these transporters, and also express MRP5 and BCRP. JC cells constitutively express Pgp and low levels of BCRP, Caco-2 cells constitutively express Pgp, MRP1 and MRP2 (**Supplementary Figure 1).**

As expected, viability of HT29/MDR cells was higher than HT29 cells after exposure to irinotecan, a substrate of Pgp (24), 5-fluorouracil, whose resistance has been associated with Pgp, MRP1 and MRP5 (25-27), and oxaliplatin, whose resistance has been associated with Pgp, MRP1and MRP4 (28, 29) (**Figure 1A, upper panels;** survival of HT29/MDR vs. HT29 cells: P=0.04 for the lowest dose of each drug, P=0.03 for the intermediate and highest doses. HT29/MDR cells were also more resistant to ER stress inducers, including thapsigargin, tunicamycin and brefeldin A (**Figure 1A, lower panels**). Chemotherapeutic drugs and ER stress inducers reduced cell number (**Figure 1B**) and growth (**Figure 1C**) in HT29 cells, but not in HT29/MDR cells (P=0.04 at 48 h; P=0.006 at 72 h; (**Figure 1B-C**).

Comparison of basal, ER stress-induced and chemotherapy-induced expression of the ER stress sensors ATF6, IRE1α, phospho(Ser724)IRE1α, PERK, phospho(Thr981)PERK, eIF2α, phospho(Ser51)eIF2α did not show any difference between HT29 and HT29/MDR cells (**Figure 2**). Triggers of ER stress and

chemotherapeutic agents induced CHOP/GADD153, TRB3, HERPUD1, cleaved caspase-3 and both C/EBP-β LAP and LIP in HT29 cells, with different kinetics (**Figure 2; Supplementary Figure 2**). By contrast, they did not induce C/EBP-β LIP, CHOP/GADD153, TRB3, HERPUD1 and cleaved caspase-3 in HT29/MDR cells (**Figure 2; Supplementary Figure 2**).

Since Pgp transports chemotherapeutic drugs, but also toxins and xenobiotics (13), it could potentially efflux thapsigargin, tunicamycin and brefeldin A from HT29/MDR cells. Therefore, we examined the possible role of Pgp in the ER stress-resistance phenotype of MDR cells. The Pgp inhibitor verapamil restored the intracellular accumulation of rhodamine 123 and doxorubicin in HT29/MDR cells (**Supplementary Figure 3A**), but did not restore the toxicity of the ER stress inducers (**Supplementary Figure 3B**), indicating that the increased activity of Pgp in HT29/MDR cells does not explain the resistance to ER stress-triggered cell death.

Thapsigargin, tunicamycin and brefeldin A modulate ABC transporters activity and expression (15, 30-32). Nevertheless, we found that in HT29 and HT29/MDR cells these agents did not change the efflux activity of Pgp, did not compete with rhodamine 123 for the efflux through Pgp and did not change the expression of *Pgp*, *MRP1* and *MRP2* at the mRNA and protein levels (**Supplementary Figure 4**, **Figure 2**). Hence, the increased resistance of HT29/MDR cells to ER stress was not due to increased efflux of these ER stress inducers, neither was it due to higher expression of Pgp. The same dual resistance to chemotherapeutic drugs, and to ER stress inducers was observed also with A549/MDR cells, with the constitutively chemoresistant JC cells and with Caco-2 cells. For each cell type, we studied the chemotherapeutic agent that serves as first line treatment choice of the respective tumor type. Importantly, each cell type exhibited a different C/EBP-β LIP/LAP ratio (data not shown).

C/EBP-β gene expression is regulated by many distinct transduction pathways, transcriptional inducers and repressors (33). Such multiplicity of regulatory cues may explain the differences in C/EBP-β LAP expression levels in the different cell types. In contrast with C/EBP-β LAP, ER stress and chemotherapy did not trigger considerable induction of C/EBP-β LIP in the drug-resistant cells. This behavior led us to hypothesize that the C/EBP-β LIP/LAP ratio serves as a key mediator of the resistance to chemotherapy and to ER stress.

The Role of LIP/LAP Ratio in the Cellular Response to ER Stress and Chemotherapy

To verify the role of LAP/LIP ratio in drug resistance, we focused on HT29/MDR cells and on JC cells, two models of acquired and constitutive MDR, respectively, and with clearly detectable levels of C/EBP-β LAP and Pgp.

First, we overexpressed C/EBP-β LAP in chemosensitive HT29 cells (**Figure 3A, upper panel**) and C/EBP-β LIP in chemoresistant HT29/MDR cells (**Figure 3A, lower panel**). LAP overexpression increased cell viability of control HT29 cells and prevented cell death induced by brefeldin A (cell survival: mean±SD =110.5±8.9%), irinotecan (cell survival: mean±SD =91.8±3.2%), 5-fluorouracil (cell survival: mean±SD =95.7±3.3%) and oxaliplatin (cell survival: mean±SD =95.0±2.5%), $P \leq 0.04$ vs. un-transfected cells in all these experimental conditions (**Figure 3B-C, left panels**). However, LAP over-expression did not affect the viability of drug-treated HT29/MDR cells (**Supplementary Figure 5**). In contrast, LIP overexpression sensitized HT29/MDR cells to brefeldin A (cell survival: mean±SD =54.7±2.7%), irinotecan (cell survival: mean±SD =48.8±2.1%), 5-fluorouracil (cell survival: mean±SD =56.0±5.5%) and oxaliplatin (cell survival: mean±SD =53.4±3.7%, $P \leq 0.04$ vs. un-transfected cells in all these experimental conditions; **Figure 3B-C, right panels**).

We next generated HT29/MDR clones stably expressing a doxycycline-inducible C/EBP-β LIP ("HT29/MDR TetON LIP" cells). Induction of LIP increased the expression of CHOP, TRB3 and cleaved caspase-3 (**Figure 4A**) and reduced cell viability (**Figure 4B**). LIP induction decreased cell proliferation as measured at 72 h (mean±SD =197,000±10,000 vs. =256,000±4,000 cells, P=0.01). LIP induction attenuated drug resistance and increased their susceptibility to ER stress triggered cell death as measured at 72 h (Brefeldin A: mean±SD =95,000±10,000 vs. 235,000±13,000, P=0.001); (irinotecan: mean±SD =85,000±11,000 vs. 247,000±13,000 cells, P<0.001; 5-fluorouracil: mean±SD =116,000±10,000 vs. 240,000±10,000 cells, P=0.002; oxaliplatin: mean±SD =136,000±11,000 vs. 257,000±12,000 cells, P=0.003; **Figure 4C**). LIP induction did not modify the cell cycle distribution of HT29/MDR cells, with the exception of the increased percentage of cells in sub-G1 phase (13.0±3.0% with doxycycline vs. 5.0±1.0% cells without doxycycline; P=0.04; **Supplementary Figure 6**), suggestive of enhanced apoptosis.

Doxycycline-mediated induction of LIP in HT29/MDR TetON LIP cells up-regulated mRNA expression of *CHOP*, *TRB3*, *PUMA, BIM*, *P62, ATG5, ATG10* and down-regulated the expression of *ATF4*, *GADD34*, *ASNS, SNAT2, CAT1, NARS*, *BCL2*, *HMOX1*, *ATG3, ATG12, MAP1LC3B* (P<0.001 for induced vs. un-induced cells for all of these genes**; Supplementary Figure 7A**). This pattern of gene expression confirmed earlier observations (34, 35), which attributed to C/EBP-β LIP a role in inducing apoptosis, controlling the UPR, autophagy, amino acid and protein synthesis/metabolism and redox regulation (**Supplementary Figure 7B**). The ER stress inducer brefeldin A further increased the expression of C/EBP-β LIP in the HT29/MDR TetON LIP clone (**Figure 4A**), thereby augmenting LIP activities. In the absence of doxycycline, brefeldin A, which

did not induce C/EBP-β LIP in HT29/MDR cells (**Figure 4A**), did not modify statistically significantly the expression of the above mentioned genes (**Supplementary Figure 7A**).

Transient over-expression of C/EBP-β LAP in HT29 cells elevated Pgp mRNA level by 3.54-fold (P<0.001, **Figure 5A**) and protein (**Figure 5C**), and increased the resistance to the Pgp substrates vinblastine (cell survival: mean±SD =87.0±5.1% vs. 61.2±7.1%, P=0.04); and etoposide (cell survival: mean±SD =81.2±5.1% vs. 43.1±7.0%, P=0.008; **Figure 5D**). By contrast, transient or stable over-expression of C/EBP-β LIP in HT29/MDR cells down-regulated Pgp mRNA levels by 4.2- and 4.73-fold (P<0.001), respectively, (**Figure 5A, B**), as well as Pgp protein (**Figure 5C**). Similar results were obtained with vinblastine (Transient LIP over-expression: Mean±SD =52.8±7.2 % vs. 92.3±7.2%, P=0.02; inducible LIP over-expression: mean±SD =42.1±3.4% vs. 90.3±5.3%, P=0.004). These cells exhibited similar responses to etoposide as well (Transient LIP over-expression: mean±SD =41.2±4.3% vs. 91.3±4.7%, P=0.008; inducible LIP over-expression: mean±SD =43.0±3.2% vs. 89.1±2.2%, P=0.003) (**Figure 5D**).

Stable over-expression of LIP in the constitutively chemoresistant JC cells activated the CHOP/TRB3/capsase-3 axis in response to tunicamycin, doxorubicin or paclitaxel, and also down-regulated C/EBP-β LAP (**Supplementary Figure 8A**). LIP over-expression decreased survival of tunicamycin-treated JC cells (mean±SD =31.2±2.2% vs. 88.3±4.3%, P=0.002); of doxorubicin-treated cells: (mean±SD =59.1±4.2% vs. 89.6±3.3%, P=0.01); and of paclitaxel-treated cells (mean±SD =46.3±3.4% vs. 81.7±2.9%, P=0.009) (**Supplementary Figure 8B, C**). Similarly, LIP over-expression decreased the replication rate (measured at 72 h) of tunicamycin-treated JC cells (mean±SD =46,000±8,000 vs. 334,000±14,000 cells, P<0.001); of doxorubicin-treated cells (mean±SD = 107,000±12,000 vs. 367,000±4,000 cells, P<0.001; and of paclitaxel-treated cells (mean±SD =75,000±14,000 vs. 325,000±10,000 cells, P<0.001) (**Supplementary Figure**

8D). In parallel, LIP over-expression reduced Pgp expression by 34.0% (P=0.04), and increased doxorubicin intracellular retention (**Supplementary Figure 8E-G**).

To study the impact of C/EBP-β LIP on drug resistance in vivo, we orthotopically implanted JC TetON LIP cells in BALB/c mice, treated them with vehicle or doxorubicin, with or without doxycycline in the drinking water. Doxorubicin alone had little effect on the tumor mass; induction of C/EBP-β LIP by doxycycline was sufficient to reduce tumor progression, and doxorubicin further reduced tumor size in animals receiving doxycycline (mean±SD =401±137 mm^3 vs. 1,570±167 mm^3 in untreated animals at day 15, P<0.001; **Figure 6A, B**). Doxorubicin alone did not reduce statistically significantly the extent of cell proliferation and did not induce detectable signs of ER stress, as determined by immunostaining of Ki67 and HERPUD1, but up-regulated Pgp in tumors, leading to drug resistance (**Figure 6C, D**). Induction of C/EBP-β LIP reduced tumor cell proliferation and increased ER stress, without affecting Pgp levels. The extent of tumor cell proliferation in mice receiving both doxycycline and doxorubicin was similar to that of doxycycline alone, whereas the extent of ER stress was further increased as determined by the ER stress marker HERPUD1. Induction of Pgp by doxorubicin was reduced upon doxycycline-mediated induction of LIP, thereby providing one mechanism by which LIP might augment the cytotoxic activity of doxorubicin (**Figure 6C, D**).

Post-Transcriptional Regulation of C/EBP-β LIP

We then investigated the molecular mechanisms underlying the lack of C/EBP-β LIP in chemotherapy-treated MDR cells. Sequencing of genomic *C/EBP-β* revealed that the chemosensitive HT29 cells and the chemoresistant HT29/MDR cells had identical DNA sequence in the ORF, 5'-UTR, 3'-UTR and promoter regions (data not shown).

To check the stability of C/EBP-β mRNA or protein, we then treated HT29 and HT29/MDR cells with the transcription inhibitor actinomycin D, which time-dependently

decreased C/EBP-β mRNA, both in the absence or presence of irinotecan. C/EBP-β LAP protein also showed a progressive decrease, without appreciable differences between HT29 and HT29/MDR cells. LIP, which was induced by irinotecan in chemosensitive cells, progressively decreased in response to actinomycin D, but was undetectable in HT29/MDR cells at all time points. A similar trend was observed in HT29 and HT29/MDR cells treated with the translation inhibitor cycloheximide. These results excluded that chemosensitive and chemoresistant cells differed in the stability of their C/EBP-β mRNA or protein (data not shown).

We found that the expression of ER quality control (ERQC) genes, often associated with increased protein ubiquitination (36), was attenuated in both HT29/MDR and A549/MDR cells (data not shown). Therefore, we compared the extent of C/EBP-β LAP and LIP ubiquitination in chemosensitive vs. MDR cells. Indeed, C/EBP-β LIP mono-ubiquitination was 3.56 fold higher in MDR cells compared with the chemosensitive cells ($P<0.001$), whereas the same level of mono-ubiquitinated C/EBP-β LAP was observed in these cells **(Figure 7A**). Inhibition of lysosomal degradation by leupeptin or ammonium chloride as well as inhibition of proteasomal degradation by MG132 prevented the disappearance of C/EBP-β LIP in the MDR cells (**Figure 7B, C, right panels**). Irinotecan did not change the extent of C/EBP-β LIP mono-ubiquitination, however, it increased C/EBP-β LAP poly-ubiquitination (**Figure 7B, C, left panels**).

The impact of C/EBP-β LIP Degradation on the MDR Phenotype

To further study the role of C/EBP-β LIP in the MDR phenotype we studied the impact of lysosomal and proteasomal inhibitors on Pgp expression and the cellular resistance to inducers of ER stress and to chemotherapy. Both NH_4Cl and MG132 partially restored the cytotoxicity of the ER stress inducer brefeldin A in the ER stress-resistant HT29/MDR cells and their combination resulted in full recovery of the cytotoxic response (survival:

mean±SD =47.3±4.7% vs. 90.5±4.5%, *P*=0.02; **Figure 7D**). In parallel, these inhibitors down-regulated the basal level of Pgp mRNA by 3.7 fold (*P*<0.001), as well as the Pgp protein level in the HT29/MDR cells (**Figure 7E, F**). Similarly, these inhibitors restored the cytotoxic response of HT29/MDR cells to irinotecan (survival: mean±SD =55.4±5.3% vs. 93.1±3.6%, *P*=0.007; **Figure 7G**).

The role of C/EBP-β LIP in Resistance to ER stress and Chemoresistance in Primary Tumors

To analyze the role of C/EBP-β LIP in primary resistant human tumors of different origin, we analyzed 3 samples of pleural malignant mesothelioma, 3 samples of glioblastoma multiforme, 3 samples of chronic lymphocytic leukemia, chosen for their constitutively high levels of Pgp (**Figure 8A**). C/EBP-β LAP was expressed in all samples whereas only low levels of C/EBP-β LIP were found (**Figure 8A**). These cells were resistant to the ER stress inducer brefeldin A and to doxorubicin (**Figure 8B**). Furthermore, triggering of ER stress with brefeldin A did not induce C/EBP-β LIP in these cells (**Figure 8C**). Over-expression of C/EBP-β LIP down-regulated Pgp (**Figure 8D)** and restored the cytotoxic efficacy of brefeldin A and doxorubicin (*P*=0.003 and 0.004, respectively, **Figure 8E**). A similar increase in C/EBP-β LIP, reduced Pgp expression (**Figure 8D)** and increased response to brefeldin A and doxorubicin was obtained by inhibiting proteasomal and lysosomal degradation using NH_4Cl plus MG132 (*P*=0.004 and *P*=0.003, respectively, **Figure 8E**).

DISCUSSION

Tumor cell adaptation to ER stress requires activation of UPR-associated pro-survival mechanisms and attenuation of UPR-associated death-promoting mechanisms, such as those triggered by C/EBP-β LIP (2, 18). LIP is necessary for promoting the nuclear translocation of CHOP (35), thereby activating the pro-apoptotic axis (4). Earlier studies

demonstrated that both chemotherapy and ER stress induce Pgp (13, 15, 16) and over-expression of C/EBP-β LIP lowers Pgp levels in MDR cells (19). Our finding that MDR cells lack CHOP and cleaved caspase 3 suggest that continuous ER stress due to limited vasculature or to chemotherapy selects for cells lacking C/EBP-β LIP. Our LIP complementation experiment suggests that loss of LIP drives the MDR phenotype by two mechanisms: it increases Pgp expression but also reduces ER stress-triggered cell death.

Our findings show that the absence of C/EBP-β LIP rather than the C/EBP-β LIP/LAP ratio is a major trigger of the MDR phenotype. Interestingly, complementation of LIP not only restored the cytotoxic effects of Pgp substrates but also that of the MRP substrates 5-fluorouracil and oxaliplatin, which also induce ER stress (5, 7, 13, 26, 27, 29, 37). Hence, LIP is probably involved in additional death-promoting mechanisms triggered by these MRP substrates. Several studies have previously shown that MDR cells are also resistant to the ER stress inducer thapsigargin. We found that these cells were also resistant to tunicamycin and brefeldin A, two ER stress inducers that are not Pgp substrates and in fact were reported to reverse the Pgp-mediated MDR (38, 39). C/EBP-β LIP was recently shown to promote pro-survival mechanisms (40, 41), however, these studies did not address its impact on the cellular response to ER stress or to chemotherapy.

C/EBP-β LIP is ubiquitinated and degraded by the proteasome in the early phase of the UPR, whereas it escapes degradation in the late phase (34, 35). Mono-ubiquitinated proteins undergo lysosomal degradation (42-45), an event commonly taking place during late ER stress (46). Hence, our finding that C/EBP-β LIP was subjected to higher basal mono-ubiquitination in HT29/MDR cells as compared with HT29 cells provides a plausible mechanism driving its loss in MDR cells. Cathepsin L inhibitors were found to overcome resistance to tamoxifen, flutamide, doxorubicin, imatinib and tricostatin by blocking lysosomal degradation of the respective target proteins (47). In addition, it was

suggested that ER stress renders cells more resistant to camptothecin and doxorubicin by increasing the degradation of topoisomerase I and II, an effect that was prevented by proteasome inhibitors (48). Since doxorubicin, etoposide, imatinib, and the active metabolites of camptothecin and tamoxifen are effluxed by Pgp, our study provides an additional mechanism of MDR reversal based on the regulation of the Pgp level by cathepsin L inhibitors. C/EBP-β LAP and LIP were also poly-ubiquitinated to some extent, suggesting that their level is regulated both by lysosomal and proteasomal degradation. Our findings were demonstrated using several resistant cell lines and three resistant primary tumor cells. Nevertheless, the reproducibility in several in vitro systems, which are accessible by other scientists is not given; validation of our conclusions based on three samples per tumor entity can provide a trend at best.

In conclusion, we propose that loss of LIP by lysosomal and proteasomal degradation following its early ubiquitination drives the MDR by two independent mechanisms: up-regulation of Pgp and attenuation of ER stress-triggered apoptosis. Since C/EBP-β LIP down-regulates tumor progression (18) and improves the therapeutic benefits of Pgp substrates, preventing its lysosomal degradation may be an effective tool to overcome drug resistance. Our findings were demonstrated using several resistant cell lines and three resistant primary tumor cells. Nevertheless, the reproducibility in several in vitro systems, which are accessible by other scientists is not given; validation of our conclusions based on three samples per tumor entity can provide a trend at best.

Funding

This work was supported by grants from De Benedetti-Cherasco Foundation (Torino - Weizmann Collaborative Program: Scientific Cooperation and Exchange); The Italian

Association for Cancer Research (AIRC; grants MFAG 11475 and IG 15232) to CR; The Estate of Sophie Kalina and The Israel Science Foundation (No. 425/12) to MR.

Notes

JK is a fellow of the Italian Foundation for Cancer Research (FIRC). MR is the Edna & Maurice Weiss Professor of Cytokine Research. The study sponsors had no role in the design of the study; the collection, analysis, and interpretation of the data; the writing of the manuscript; and the decision to submit the manuscript for publication.

We thank Dr. Roberta Libener and Dr. Sara Orecchia, Biologic Bank of Malignant Mesothelioma, Santi Antonio e Biagio Hospital, Alessandria, Italy; Prof. Davide Schiffer and Dr. Marta Mellai, Neuro-Bio-Oncology Center, Vercelli, Italy; Prof. Massimo Massaia and Dr. Marta Coscia, Hematology Division, San Giovanni Battista Hospital, Torino, Italy, for having provided the primary tumor samples analyzed in the study.

References

1. Kim I, Xu W, Reed J. Cell death and endoplasmic reticulum stress: Disease relevance and therapeutic opportunities. *Nat Rev Drug Discov*. 2008;7(12):1013-1030.

2. Rutkowski D, Kaufman R. That which does not kill me makes me stronger: Adapting to chronic er stress. *Trends Biochem Sci*. 2007;32(10):469-476.

3. Hanahan D, Weinberg R. Hallmarks of cancer: The next generation. *Cell* 2011;144(5):646-674.

4. Ohoka N, Yoshii S, Hattori T, Onozaki K, Hayashi H. Trb3, a novel er stress-inducible gene, is induced via atf4-chop pathway and is involved in cell death. *Embo J*. 2005;24(6):1243-1255.

5. Panaretakis T, Kepp O, Brockmeier U*, et al.* Mechanisms of pre-apoptotic calreticulin exposure in immunogenic cell death. *Embo J*. 2009;28(5):578-590.

6. Mandic A, Hansson J, Linder S, Shoshan M. Cisplatin induces endoplasmic reticulum stress and nucleus-independent apoptotic signaling. *J Biol Chem*. 2003;278(11):9100-9106.

7. Yadunandam A, Yoon J, Seong Y, Oh C, Kim G. Prospective impact of 5-fu in the induction of endoplasmic reticulum stress, modulation of grp78 expression and autophagy in sk-hep1 cells. *Int J Oncol*. 2012;41(3):1036-1042.

8. Mhaidat N, Alali F, Matalqah S*, et al.* Inhibition of mek sensitizes paclitaxel-induced apoptosis of human colorectal cancer cells by downregulation of grp78. *Anti-Cancer Drugs* 2009;20(7):601-606.

9. Moenner M, Pluquet O, Bouchecareilh M, Chevet E. Integrated endoplasmic reticulum stress responses in cancer. *Cancer Res*. 2007;67(22):10631-10634.

10. Dorard C, de Thonel A, Collura A*, et al.* Expression of a mutant hsp110 sensitizes colorectal cancer cells to chemotherapy and improves disease prognosis. *Nat Med*. 2011;17(10):1283-1289.

11. Maddalena F, Laudiero G, Piscazzi A*, et al.* Sorcin induces a drug-resistant phenotype in human colorectal cancer by modulating ca2+ homeostasis. *Cancer Res*. 2011;71(24):7659-7669.

12. Holohan C, Van Schaeybroeck S, Longley DB, Johnston PG. Cancer drug resistance: An evolving paradigm. *Nat Rev Cancer* 2013;13(10):714-726.

13. Gottesman M, Fojo T, Bates S. Multidrug resistance in cancer: Role of atp-dependent transporters. *Nat Rev Cancer* 2002;2(1):48-58.

14. Bi M, Naczki C, Koritzinsky M*, et al.* Er stress-regulated translation increases tolerance to extreme hypoxia and promotes tumor growth. *Embo J*. 2005;24(19):3470-3481.

15. Ledoux S, Yang R, Friedlander G, Laouari D. Glucose depletion enhances p-glycoprotein expression in hepatoma cells: Role of endoplasmic reticulum stress response. *Cancer Res*. 2003;63(21):7284-7290.

16. O'Donnell JL, Joyce MR, Shannon AM*, et al.* Oncological implications of hypoxia inducible factor-1alpha (hif-1alpha) expression. *Cancer Treat Rev*. 2006;32(6):407-416.

17. Descombes P, Schibler U. A liver-enriched transcriptional activator protein, lap, and a transcriptional inhibitory protein, lip, are translated from the same messenger-rna. *Cell* 1991;67(3):569-579.

18. Meir O, Dvash E, Werman A, Rubinstein M. C/ebp-beta regulates endoplasmic reticulum stress-triggered cell death in mouse and human models. *Plos One* 2010;5(3):e9516.

19. Chen G, Sale S, Tan T, Ermoian R, Sikic B. Ccaat/enhancer-binding protein beta (nuclear factor for interleukin 6) transactivates the human mdr1 gene by interaction with an inverted ccaat box in human cancer cells. *Mol Pharm*. 2004;65(4):906-916.

20. Riganti C, Miraglia E, Viarisio D*, et al.* Nitric oxide reverts the resistance to doxorubicin in human colon cancer cells by inhibiting the drug efflux. *Cancer Res*. 2005;65(2):516-525.

21. Lee B, French K, Zhuang Y, Smith C. Development of a syngeneic in vivo tumor model and its use in evaluating a novel p-glycoprotein modulator, pgp-4008. *Oncol Res*. 2003;14(1):49-60.

22. Lo YL, Ho CT, Tsai FL. Inhibit multidrug resistance and induce apoptosis by using glycocholic acid and epirubicin. *Eur J Pharm Sci*. 2008;35(1-2):52-67.

23. Shan S, Sorg B, Dewhirst MW. A novel rodent mammary window of orthotopic breast cancer for intravital microscopy. *Microvasc Res*. 2003;65(2):109-117.

24. Rabba A, Si L, Xue K, Li M, Li G. In situ intestinal perfusion of irinotecan: Application to p-gp mediated drug interaction and introduction of an improved hplc assay. *J Pharm Pharm Sci*. 2011;14(2):138-147.

25. Yao H, Duan Z, Wang M*, et al.* Adrenaline induces chemoresistance in ht-29 colon adenocarcinoma cells. *Cancer Genet Cytogenet*. 2009;190(2):81-87.

26. Jin J, Huang M, Wei H, Liu G. Mechanism of 5-fluorouracil aquired resistance in human hepatocellular carcinoma cell line bel(7402). *World J Gastroenterol*. 2002;8(6):1029-1034.

27. Hagmann W, Jesnowski R, Faissner R, Guo C, Löhr J. Atp-binding cassette c transporters in human pancreatic carcinoma cell lines. Upregulation in 5-fluorouracil-resistant cells. *Pancreatology* 2009;9(1-2):136-144.

28. Zhao Q, Zhang H, Li Y*, et al.* Anti-tumor effects of cik combined with oxaliplatin in human oxaliplatin-resistant gastric cancer cells in vivo and in vitro. *J Exp Clin Cancer Res.* 2010;29:118.

29. Beretta G, Benedetti V, Cossa G*, et al.* Increased levels and defective glycosylation of mrps in ovarian carcinoma cells resistant to oxaliplatin. *Biochem Pharmacol*. 2010;79(8):1108-1117.

30. Seres M, Ditte P, Breier A, Sulova Z. Effect of thapsigargin on p-glycoprotein-negative and p-glycoprotein-positive l1210 mouse leukaemia cells. *Gen Physiol Biophys*. 2010;29(4):396-401.

31. Hiss D, Gabriels G, Folb P. Combination of tunicamycin with anticancer drugs synergistically enhances their toxicity in multidrug-resistant human ovarian cystadenocarcinoma cells. *Cancer Cell Int*. 2007;7:5.

32. Fu D, Bebawy M, Kable E, Roufogalis B. Dynamic and intracellular trafficking of p-glycoprotein-egfp fusion protein: Implications in multidrug resistance in cancer. *Int J Cancer* 2004;109(2):174-181.

33. Huber R, Pietsch D, Panterodt T, Brand K. Regulation of C/EBPβ and resulting functions in cells of the monocytic lineage. *Cell Signal*. 2012;24(6):1287-1296.

34. Li Y, Bevilacqua E, Chiribau C*, et al.* Differential control of the ccaat/enhancer-binding protein beta (c/ebp beta) products liver-enriched transcriptional activating protein (lap) and liver- enriched transcriptional inhibitory protein (lip) and the regulation of gene expression during the response to endoplasmic reticulum stress. *J Biol Chem*. 2008;283(33):22443-22456

35. Chiribau C, Gaccioli F, Huang C, Yuan C, Hatzoglou M. Molecular symbiosis of chop and c/ebp beta isoform lip contributes to endoplasmic reticulum stress-induced apoptosis. *Mol Cell Biol*. 2010;30(14):3722-3731.

36. Vembar S, Brodsky J. One step at a time: Endoplasmic reticulum-associated degradation. *Nat Rev Mol Cell Biol*. 2008;9(12):944-957.

37. Agarwal S, Sane R, Oberoi R, Ohlfest J, Elmquist W. Delivery of molecularly targeted therapy to malignant glioma, a disease of the whole brain. *Exp Rev Mol Med.* 2011;13:e17.

38. Kramer R, Weber TK, Arceci R*, et al.* Inhibition of n-linked glycosylation of p-glycoprotein by tunicamycin results in a reduced multidrug resistance phenotype. *Br J Cancer* 1995;71(4):670-5.

39. Fu D, Bebawy M, Kable EPW, Roufogalis BD. Dynamic and intracellular trafficking of p-glycoprotein-egfp fusion protein: Implications in multidrug resistance in cancer. *Int J Cancer* 2004;109(2):174-181.

40. Saint-Auret G, Danan J, Hiron M*, et al.* Characterization of the transcriptional signature of c/ebpbeta isoforms (lap/lip) in hep3b cells: Implication of lip in pro-survival functions. *J Hepatol*. 2011;54(6):1185-1194.

41. Li H, Baldwin B, Zahnow C. Lip expression is regulated by igf-1r signaling and participates in suppression of anoikis. *Mol Cancer* 2011;10:100.

42. Haglund K, Sigismund S, Polo S*, et al.* Multiple monoubiquitination of rtks is sufficient for their endocytosis and degradation. *Nat Cell Biol*. 2003;5(5):461-466.

43. Leithe E, Rivedal E. Ubiquitination and down-regulation of gap junction protein connexin-43 in response to 12-o-tetradecanoylphorbol 13-acetate treatment. *J Biol Chem*. 2004;279(48):50089-50096.

44. Chen B, Mallampalli R. Masking of a nuclear signal motif by monoubiquitination leads to mislocalization and degradation of the regulatory enzyme cytidylyltransferase. *Mol Cell Biol*. 2009;29(11):3062-3075.

45. Sun T, Guo J, Shallow H*, et al.* The role of monoubiquitination in endocytic degradation of human ether-a-go-go-related gene (herg) channels under low K+ conditions. *J Biol Chem*. 2011;286(8):6751-6759.

46. Shenkman M, Tolchinsky S, Lederkremer GZ. Er stress induces alternative nonproteasomal degradation of er proteins but not of cytosolic ones. *Cell Stress Chaperones* 2007;12(4):373-383.

47. Zheng X, Chu F, Chou P*, et al.* Cathepsin l inhibition suppresses drug resistance in vitro and in vivo: A putative mechanism. *Am. J Physiol Cell Physiol*. 2009;296(1):C65-C74.

48. Tsuruo T, Naito M, Tomida A*, et al.* Molecular targeting therapy of cancer: Drug resistance, apoptosis and survival signal. *Cancer Sci*. 2003;94(1):15-21.

FIGURE LEGENDS

Figure 1. Effects of Chemotherapy and ER Stress Inducers on Chemosensitive and Chemoresistant Cells. **A**) Human chemosensitive colon cancer HT29 cells and chemoresistant HT29/MDR cells were incubated for 48 h in the absence (0) or presence of increasing concentrations of irinotecan (CPT11), 5-fluorouracil (5FU), oxaliplatin (oPt), thapsigargin (Tg), tunicamycin (Tu), brefeldin A (Bfa). Cell viability was assessed in quadruplicate by neutral red staining. Data are presented as means±SD (n=4). *$P \leq 0.03$, ≤ 0.006 and ≤ 0.006 for cells treated with low, intermediate or high doses of the various agents vs. untreated ("0") cells. °$P \leq 0.04$, ≤ 0.03 and ≤ 0.03 for HT29/MDR vs. HT29 cells treated with low, intermediate or high doses of the various agents (two-sided ANOVA). **B**) Cells (10^5/well) were grown for 48 h in 96-well plates in media without (Ctrl) or with irinotecan (10 µM), 5-fluorouracil (5 µM), oxaliplatin (5 µM), thapsigargin (50 nM), tunicamycin (1 µM) or brefeldin A (50 nM), then stained with crystal violet and photographed (upper panels, 1x; lower panels, bright field microscopy). For each experimental point, a minimum of 5 microscopic fields were examined. Bars = 500 µM. **C**) Cells (50,000/well) were cultured in 96-well plates, in media without (Ctrl) or with the indicated agents at concentrations as in B. Cell counts were determined in quadruplicate following fixation and crystal violet staining at the indicated times. Data are presented as mean±SD (n=4). *$P < 0.001$ for all drugs: treated cells vs. untreated (Ctrl) cells; °$P \leq 0.04$ (48 h), °$P \leq 0.006$ (72 h) for HT29/MDR cells vs. HT29 cells (two-sided ANOVA).

Figure 2. Expression of ER Stress–Associated Proteins in Chemosensitive and Chemoresistant Cells Under ER stress or Chemotherapy. HT29 and HT29/MDR cells were incubated 48 h in media without (Ctrl) or with thapsigargin (50 nM, Tg),

tunicamycin (1 μM, Tun), brefeldin A (50 nM, Bfa), irinotecan (10 μM, CPT11), 5-fluorouracil (5 μM, 5FU), or oxaliplatin (5 μM, oPt). Cell extracts were resolved by SDS-PAGE and immunoblotted with specific antibodies for ATF6, IRE1α, phospho(Ser724)IRE1α, PERK, phospho(Thr980)PERK, eIF2α, phospho(Ser51)eIF2α, C/EBP-β (recognizing the common C-terminal peptide of LAP and LIP), CHOP, TRB3, HERPUD1, caspase-3 (recognizing both procaspase-3 and cleaved caspase-3), Pgp, MRP1, MRP2. An anti-actin antibody was used as a loading control.

Figure 3. The Impact of C/EBP-β LIP/LAP Ratio on Cell Viability Under ER Stress or Chemotherapy. HT29 and HT29/MDR cells (-), cells transfected with empty pcDNA4/TO vector (em), with pcDNA4/TO expression vector encoding C/EBP-β LAP or C/EBP-β LIP, were grown for 48 h in media without (Ctrl) or with brefeldin A (50 nM, Bfa), irinotecan (10 μM, CPT11), 5-fluorouracil (5 μM, 5FU) or oxaliplatin (5 μM, oPt). **A**) Extracts were resolved by SDS-PAGE and immunoblotted with a specific antibody recognizing the C-terminal peptide of C/EBPβ, which recognizes both LAP and LIP. Blotting with an anti-actin antibody served as a load control. Notice the induction of endogenous LIP in the HT29 cells, but not in the HT29/MDR cells, upon induction of ER stress and by chemotherapy. **B**) Cell viability following treatments with vehicle or the indicated agents as in A. Viability was assessed in quadruplicate by neutral red staining. Data are presented as means±SD (n=4). °$P \leq 0.04$ for the LAP expressing cells vs. un-transfected cells. *$P \leq 0.001$ for cells treated with the cytotoxic agents vs. untreated cells, °$P \leq 0.04$ for the LIP expressing cells vs. un-transfected cells and *$P \leq 0.002$ for cells treated with the cytotoxic agents vs. untreated cells (two-sided ANOVA). **C**) Cells (10^5/well) in 96-well plates were treated as in A and then stained with crystal violet and

photographed (upper panels, 1x; lower panels, bright field microscopy). For each experimental point, a minimum of 5 microscopic fields were examined. Bars = 500 µM.

Figure 4. The Impact of C/EBP-β LIP on Sensitivity of Chemoresistant cells to ER Stress and to Chemotherapy. **A**) HT29/MDR TetON LIP cells, stably transfected with the inducible pcDNA4/TO expression vector for C/EBPβ LIP, were cultured for 48 h in media without (- Doxy) or with 1 µg/ml doxycycline (+ Doxy), in the absence (Ctrl) or presence of brefeldin A (50 nM, Bfa), irinotecan (10 µM, CPT11), 5-fluorouracil (5 µM, 5FU) or oxaliplatin (5 µM, oPt). Cell extracts were resolved by SDS-PAGE and immunoblotted with specific antibodies for C/EBP-β (recognizing the C-terminal peptide), CHOP, TRB3 and caspase-3 (recognizing both procaspase-3 and cleaved caspase-3). Blotting with an anti-actin antibody served as a load control. **B**) HT29/MDR TetON LIP cells (10^5/well) were cultured in 96-well plates with the indicated agents as in A. The cells were then stained with crystal violet and photographed (upper panels, 1x; lower panels, bright field microscopy). For each experimental point, a minimum of 5 microscopic fields were examined. Bars = 500 µM. **C**) HT29/MDR TetON LIP cells (50,000/well) were cultured in 96-well plates and treated as in A. The cell number was determined following fixation and crystal violet staining in quadruplicate at the indicated times. Data are presented as mean±SD (n=4). **P*=0.04 (24 h), **P*=0.01 (48 h), **P*=0.01 (72 h) for untreated (Ctrl) "+Doxy" cells vs. untreated (Ctrl) "-Doxy" cells; °*P*=0.02 (48 h), °*P*=0.001 (72 h), for "+Doxy" cells treated with Bfa vs. "-Doxy" cells; °*P*=0.003 (48 h), °*P*<0.001 (72 h), for "+Doxy" cells treated with CPT vs. "-Doxy" cells; °*P*=0.02 (48 h), °*P*=0.002 (72 h), for "+Doxy" cells treated with 5FU vs. "-

Doxy" cells; °*P*=0.02 (48 h), °*P*=0.003 (72 h), for "+ Doxy" cells treated with oPt vs. "- Doxy" cells (two-sided ANOVA).

Figure 5. The Impact of C/EBP-β LIP on Pgp Levels. **A**) HT29 and HT29/MDR cells were either non-transfected (-), transfected with empty pcDNA4/TO vector (em), with a pcDNA4 expression vector for C/EBP-β LAP or with a pcDNA4 expression vector for C/EBP-β LIP. Total RNA was extracted at 48 h post transfection, reverse-transcribed and subjected to qRT-PCR for *Pgp, MRP1 and MRP2* genes. Measurements were performed in triplicate and data are presented as means±SD (n=3) vs. the respective untreated (-) cells: **P*<0.001, for HT29 and HT29/MDR cells overexpressing LAP or LIP vs. un-transfected cells (two-sided ANOVA). **B**) HT29/MDR cells stably transfected with the inducible pcDNA4/TO expression vector for C/EBP-β LIP (HT29/MDR TetON LIP) were grown in media without (-) or with (+) doxycycline (Doxy; 1 μg/ml) for 48 h. Total RNA was extracted, reverse-transcribed and subjected to qRT-PCR for *Pgp, MRP1 and MRP2* genes. Measurements were performed in triplicate and data are presented as means ±SD (n=3) vs. the respective untreated (-) cells: **P*<0.001 (two-sided ANOVA). **C**) Extracts of cells treated as in A and B were resolved by SDS-PAGE and immunoblotted with the indicated antibodies. Anti actin served as a load control. **D**) Cells treated as in A and B were grown for 48 h in media without (Ctrl) or with the Pgp substrates vinblastine (1 μM, Vbl) or etoposide (1 μM, Eto). Cell viability was assessed by neutral red staining. Data are presented as means±SD (n=4). **P*=0.007 for the LAP expressing cells vs. un-transfected (Ctrl, -) cells; °*P*=0.04 and 0.008 for LAP expressing cells treated with vinblastine or etoposide vs. un-transfected (-) cells. °*P*=0.04, 0.02 and 0.008 for the LIP-expressing HT29/MDR cells, either untreated, treated with vinblastine or with etoposide vs.

un-transfected (-) cells. For HT29/MDR TetON LIP cells: *P=0.02, 0.004 and 0.003 for +Doxy vs. -Doxy treated HT29/MDR TetON LIP control cells, vinblastine (Vbl)- or etoposide (Eto)-treated cells (two-sided ANOVA).

Figure 6. The impact of C/EBP-β LIP Induction on Tumor Growth In Vivo. Six weeks old female BALB/c mice bearing a 100 mm^3-tumor of constitutively chemoresistant JC TetON LIP cells were treated on days 0, 6, and 12 with saline (Ctrl) or 5 mg/kg doxorubicin (Dox) ip. LIP was induced by doxycycline (doxy) in the drinking water. Mice were euthanized on day 15. **A**) Tumor growth was monitored daily by caliper measure. Data are presented as mean±SD of 15 mice/group. *P<0.001 for "doxy" and "Dox + doxy" group vs. "Ctrl" group; °P=0.006 (day 12), °P=0.007 (day 15), for "Dox + doxy" group vs. "Dox" group. **B**) Photograph of representative tumors (two-sided ANOVA). **C**) Sections of tumors from each group of animals were stained with hematoxylin and eosin (HE) or immunostained with antibodies for Ki67 as an index of proliferation, HERPUD1 as an index of ER stress, or Pgp, followed by incubation with peroxidase-conjugated secondary antibodies. Nuclei were counter-stained with hematoxylin. Bar = 10 µm. The photograph is a representative of sections from 5 tumors. **D**) Immunostaining quantification. The percent of proliferating cells was determined by the ratio of Ki67-positive nuclei and the total cell count (hematoxylin-positive nuclei), by counting sections from 5 animals of each group (107-92 nuclei/field); "Ctrl" group percentage was considered 100%. The percentage of HERPUD1 and Pgp-positive cells was determined by analyzing sections from 5 animals of each group (109-91 cells/field), using Photoshop program. "Ctrl" group intensity was considered 100%. *P=0.007 (Ki67), *P=0.003 (HERPUD1), *P=0.005 (Pgp), for "doxy" or "Dox +

doxy" group vs. "Ctrl" group; °*P*=0.006 (Ki67), °*P*=0.002 (HERPUD1), °*P*=0.003 (Pgp), for "Dox + doxy" group vs. "Dox" group (two-sided ANOVA).

Figure 7. The Impact of Proteasome and Lysosome Inhibitors on Resistance to ER stress and Chemotherapy. **A**) Extracts from HT29 and HT29/MDR cells were immunoprecipitated (IP) with an anti-C/EBP-β antibody (recognizing the common C-terminal peptide), and then immunoblotted (IB) with anti-mono/polyubiquitin (UQ) antibody or with the anti-C/EBP-β antibody. No Ab: extracts of HT29 cells precipitated in the absence of the anti-C/EBP-β antibody were used as internal control. Densitometric results were expressed as arbitrary units. **P*<0.001 for monoubiquitinated LIP; **P*=0.002 for total LIP in HT29 vs. HT29/MDR cells. (two-sided ANOVA). **B-C**) Cells were grown for 48 h in media without (-) or with irinotecan (10 μM, CP), in the absence or presence of various combinations of the proteasome inhibitor MG132 (10 μM for the last 6 h, MG), the cathepsin inhibitor leupeptin (200 μM for the last 3 h, L), or the lysosome inhibitor NH_4Cl (50 mM for the last 3 h, N). Cell extracts were then subjected to immunoprecipitation and immunoblotting as in A. **D**) HT29/MDR cells were grown 48 h in media without (-) or with brefeldin A (50 nM, Bfa), in the absence or presence of the proteasome inhibitor MG132 (10 μM for the last 6 h, MG), the lysosome inhibitor NH_4Cl (50 mM for the last 3 h, N) or both inhibitors. HT29 cells were included as controls. Cell viability was assessed in quadruplicate by neutral red staining. Data are presented as means±SD (n=4). **P*=0.014 for cells treated or not with Bfa. °*P*=0.03, 0.03 and 0.02 for cells treated with Bfa and either MG132, NH_4Cl, or MG132 and NH_4Cl vs. inhibitors only (two-sided ANOVA). **E**) HT29/MDR cells were grown in media without (-) or with MG132 (10 μM for 6 h, MG), NH_4Cl (50 mM for 3 h, N), or both agents. Untreated (-) HT29 cells were included as internal control. The cells were

then washed and grown in fresh medium for additional 24 h; total RNA was extracted, reverse-transcribed and subjected to qRT-PCR for *Pgp, MRP1* and *MRP2* mRNA. Data are presented as means±SD (n=3). For all transporters **P*<0.001 in HT29/MDR vs. HT29 cells without inhibitors. °*P*<0.001 for HT29/MDR cells treated with MG132, NH_4Cl, or MG132 plus NH_4Cl vs. no inhibitor (-; two-sided ANOVA). **F**) Cells were cultured as in B, then washed and grown in fresh medium for additional 48 h. Cell extracts were then resolved by SDS-PAGE and immunoblotted with the indicated antibodies. Anti actin served as a load control. **G**) Cells were grown 48 h in media without (-) or with irinotecan (10 μM, CP), in the absence or presence of MG132 (10 μM for the last 6 h, MG), NH_4Cl (50 mM for the last 3 h, N) or both agents. Cell viability was assessed in quadruplicate by neutral red staining. Data are means±SD (n=4). **P*=0.02 for cells treated with irinotecan vs. untreated cells (-). °*P*=0.03 and 0.02 for cells treated with irinotecan plus MG132 or NH_4Cl vs. irinotecan alone. °*P*≤0.007 for cells treated with irinotecan plus MG132 and NH_4Cl, vs. inhibitors only (two-sided ANOVA).

Figure 8. The Impact of LIP Expression on Response of Primary Resistant Tumor Cells to ER Stress and Chemotherapy. **A**) Immunoblot analysis with anti Pgp and anti C/EBP-β (recognizing the C-terminal peptide), performed with extracts from primary tumor cells isolated from 3 malignant mesothelioma (MM), 3 glioblastoma multiforme (GBM) and 3 chronic lymphocytic leukemia (CLL) patients. UPN is Unknown Patient Number. Anti actin served as a load control. **B**) Cells shown in A) were cultured for 48 h in media without (-) or with brefeldin A (50 nM, Bfa) or doxorubicin (5 μM, Dox). Cell viability was assessed in quadruplicate by neutral red staining. Data are presented as means±SD (n=4). **C**) Cells of UPN 1, 6 and 9 were cultured for 48 h in media without (-) or with (+) brefeldin A (50 nM, Bfa).

Immunoblot analysis with anti C/EBP-β of the cell extracts are shown. Anti actin served as a load control. **D**) Cells of patients shown in C), were either left untreated (-), transfected with the pcDNA4/TO expression vector encoding C/EBP-β LIP (LIP), or treated with both MG132 (10 μM, 6 h, MG) and NH_4Cl (50 mM 3 h, N). Immunoblots with anti C/EBP-β and anti Pgp are shown. Anti actin served as a load control. **E**) The same cell isolates were treated as in D, cultured for 48 h in fresh media (Ctrl), media containing brefeldin A (50 nM, Bfa) or doxorubicin (5 μM, Dox). Cell viability was assessed by neutral red staining. Data are presented as means±SD (n=4). For LIP over-expressing cells of all patients *P≤0.04, ≤0.003 and ≤0.004 for control, Bfa and Dox-treated cells vs. un-transfected cells (-). For cells of all patients treated with MG132 and NH_4Cl, together with Bfa or Dox *P≤0.004 and ≤0.003 vs. untreated (-) cells, respectively. For LIP over-expressing cells of all patients, treated with Bfa or Dox °P≤0.008 and ≤0.009 vs. un-transfected cells treated with Bfa or Dox, respectively. For cells of all patients, treated with MG132 and NH_4Cl and either Bfa or Dox °P≤0.006 and ≤0.007 vs. cells treated with Bfa or Dox alone, respectively (two-sided ANOVA).

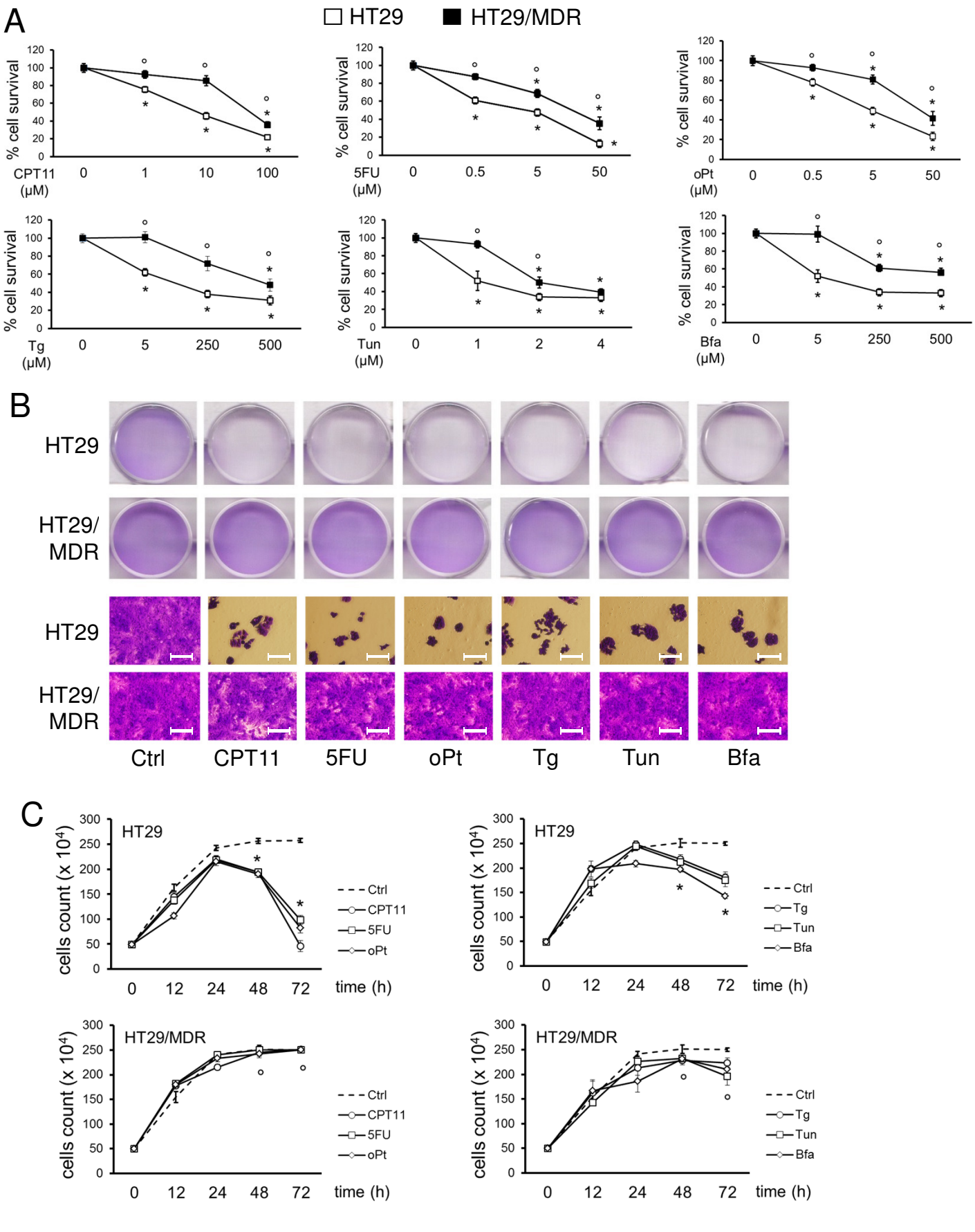
A
HT29
HT29/MDR
% cell survival
CPT11 (μM)
5FU (μM)
oPt (μM)
Tg (μM)
Tun (μM)
Bfa (μM)
B
HT29
HT29/ MDR
Ctrl
CPT11
5FU
oPt
Tg
Tun
Bfa
C
cells count (x 10⁴)
time (h)
Ctrl
CPT11
5FU
oPt
Tg
Tun
Bfa

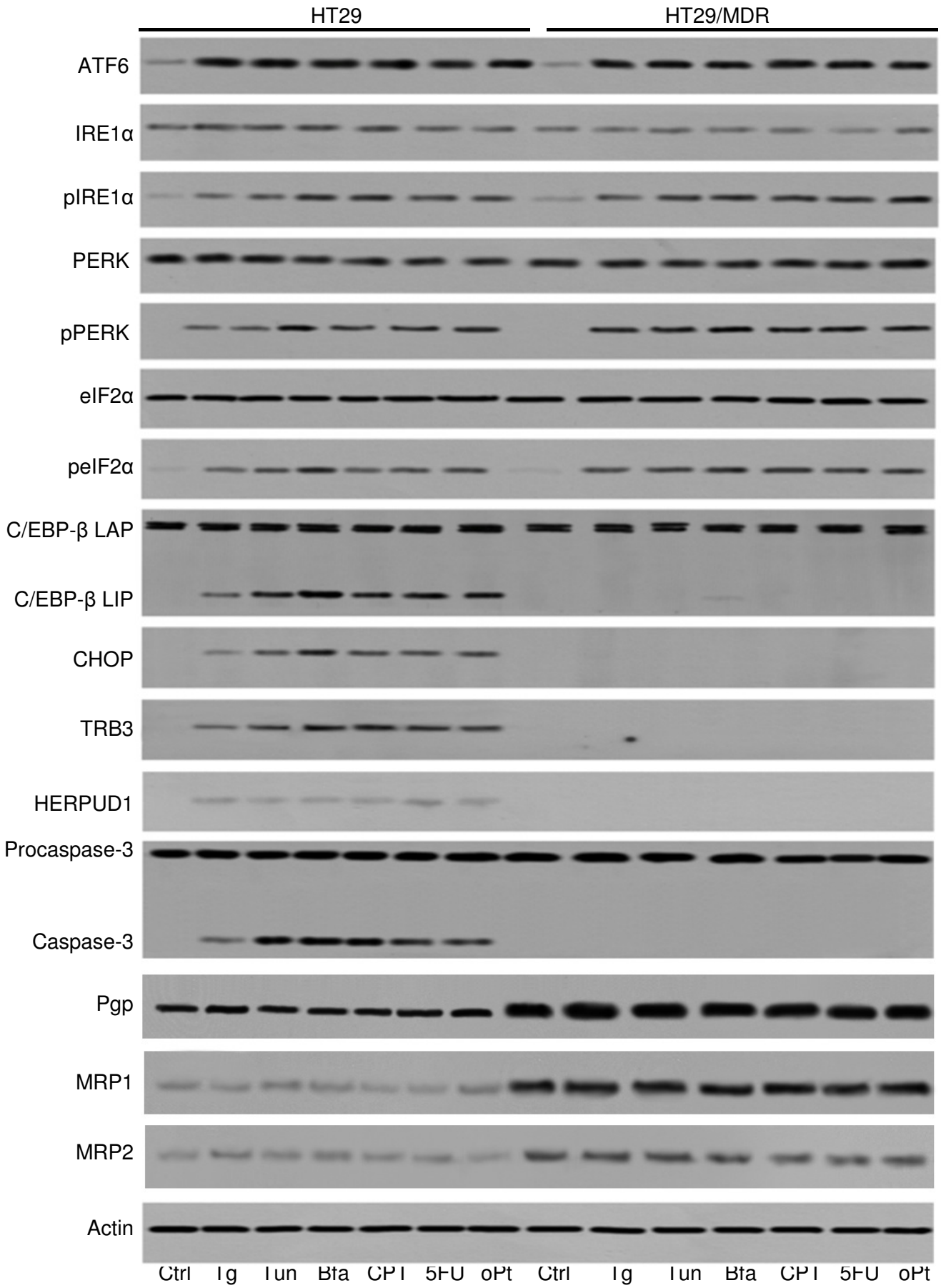
HT29
HT29/MDR
ATF6
IRE1α
pIRE1α
PERK
pPERK
eIF2α
peIF2α
C/EBP-β LAP
C/EBP-β LIP
CHOP
TRB3
HERPUD1
Procaspase-3
Caspase-3
Pgp
MRP1
MRP2
Actin
Ctrl
Tg
Tun
Bfa
CPT
5FU
oPt
Ctrl
Tg
Tun
Bfa
CPT
5FU
oPt

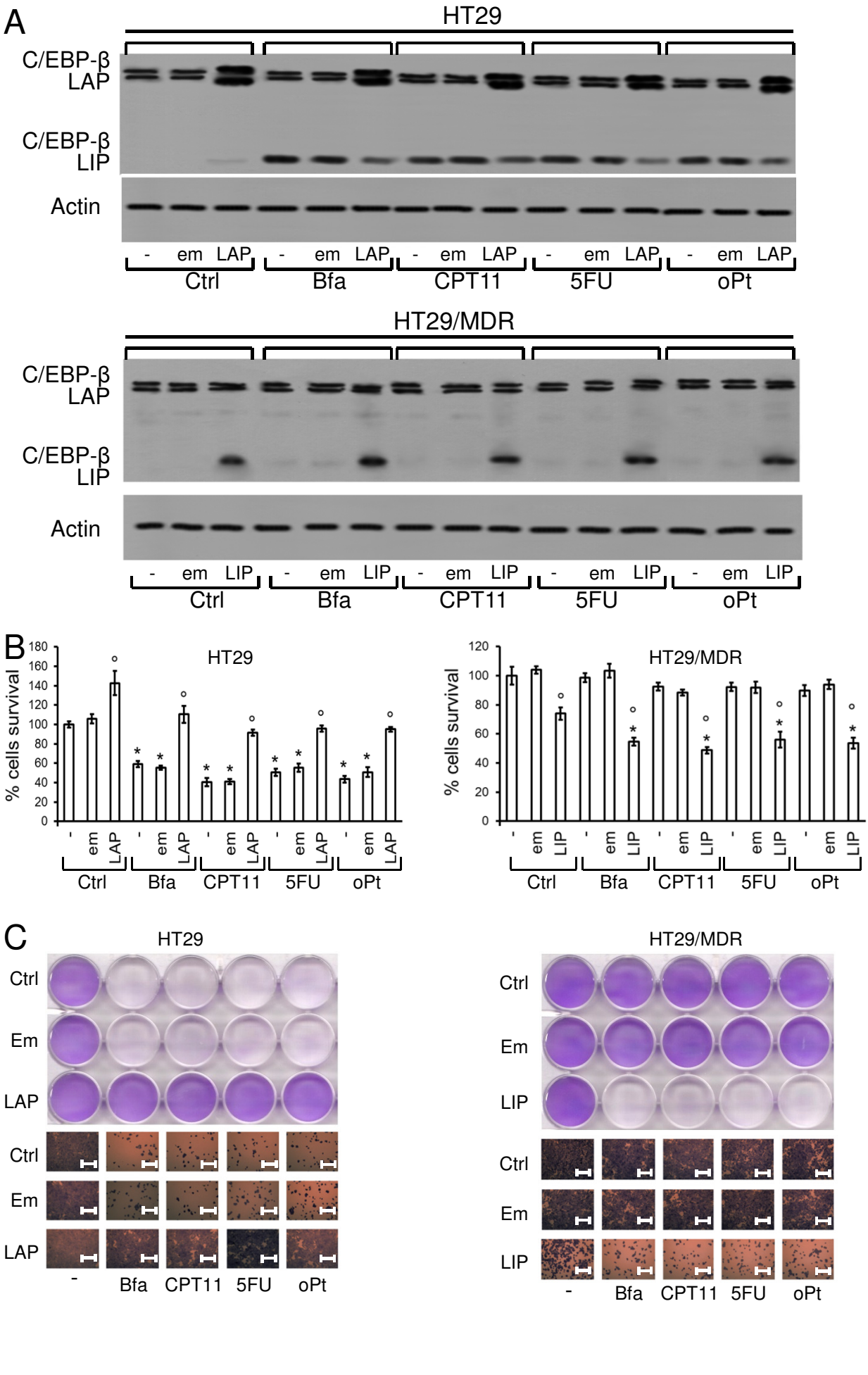
A
HT29
C/EBP-β LAP
C/EBP-β LIP
Actin
- em LAP
Ctrl
Bfa
CPT11
5FU
oPt
HT29/MDR
- em LIP
B
HT29
% cells survival
HT29/MDR
C
HT29
HT29/MDR
Ctrl
Em
LAP
LIP
Bfa
CPT11
5FU
oPt

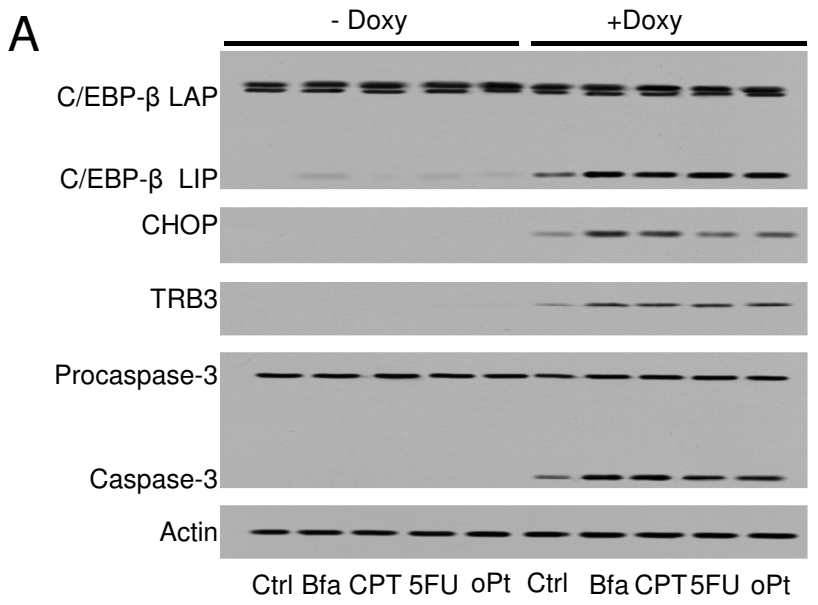
A
- Doxy
+Doxy
C/EBP-β LAP
C/EBP-β LIP
CHOP
TRB3
Procaspase-3
Caspase-3
Actin
Ctrl Bfa CPT 5FU oPt Ctrl Bfa CPT 5FU oPt

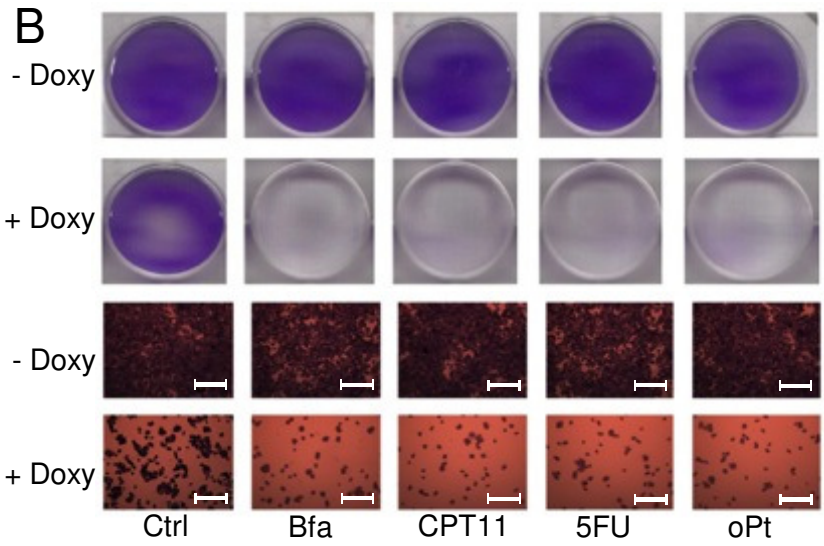
B
- Doxy
+ Doxy
- Doxy
+ Doxy
Ctrl
Bfa
CPT11
5FU
oPt

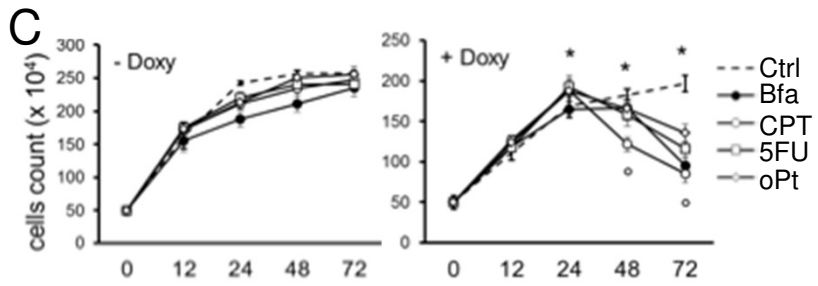
C
cells count (x 10⁴)
- Doxy
+ Doxy
0 12 24 48 72
Ctrl
Bfa
CPT
5FU
oPt

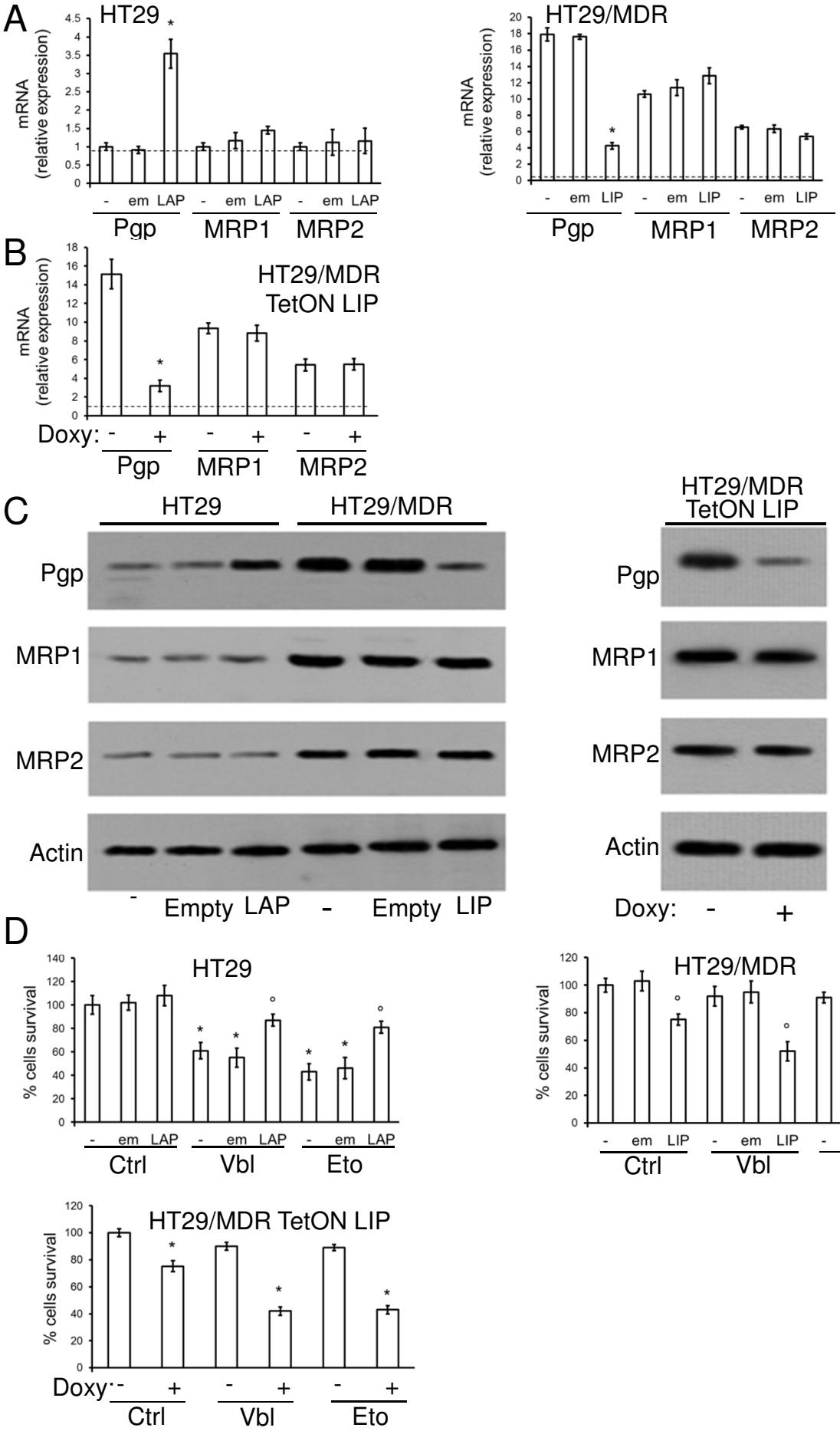
A
HT29
mRNA (relative expression)
- em LAP - em LAP - em LAP
Pgp MRP1 MRP2
HT29/MDR
- em LIP - em LIP - em LIP
Pgp MRP1 MRP2
B
HT29/MDR TetON LIP
Doxy: - + - + - +
Pgp MRP1 MRP2
C
HT29
HT29/MDR
Pgp
MRP1
MRP2
Actin
- Empty LAP - Empty LIP
HT29/MDR TetON LIP
Doxy: - +
D
HT29
% cells survival
- em LAP - em LAP - em LAP
Ctrl Vbl Eto
HT29/MDR
- em LIP - em LIP - em LIP
Ctrl Vbl Eto
HT29/MDR TetON LIP
Doxy: - + - + - +
Ctrl Vbl Eto

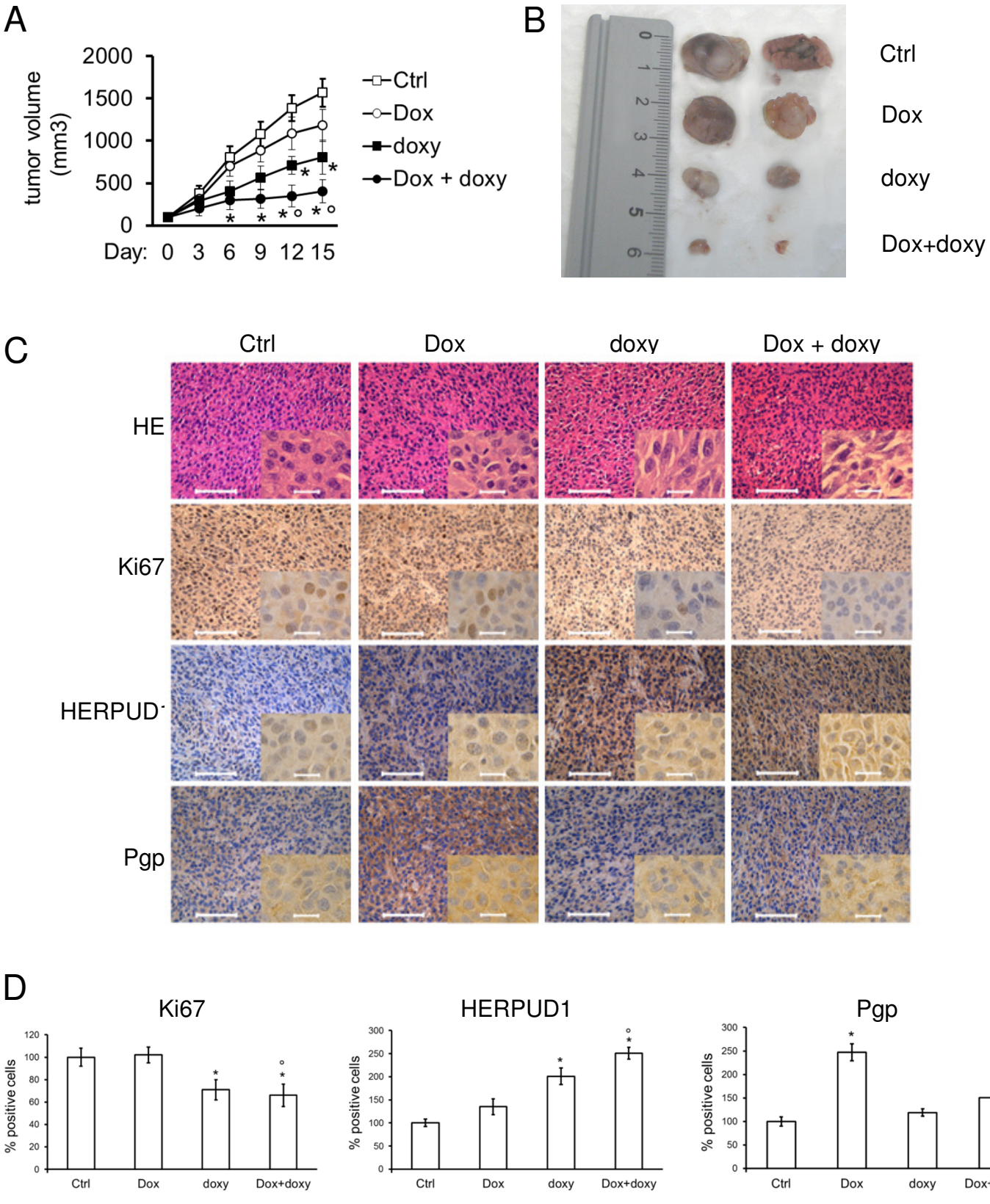
A
tumor volume (mm3)
2000
1500
1000
500
0
Day: 0 3 6 9 12 15
Ctrl
Dox
doxy
Dox + doxy
B
Ctrl
Dox
doxy
Dox+doxy
C
Ctrl
Dox
doxy
Dox + doxy
HE
Ki67
HERPUD1
Pgp
D
Ki67
HERPUD1
Pgp
% positive cells
Ctrl
Dox
doxy
Dox+doxy

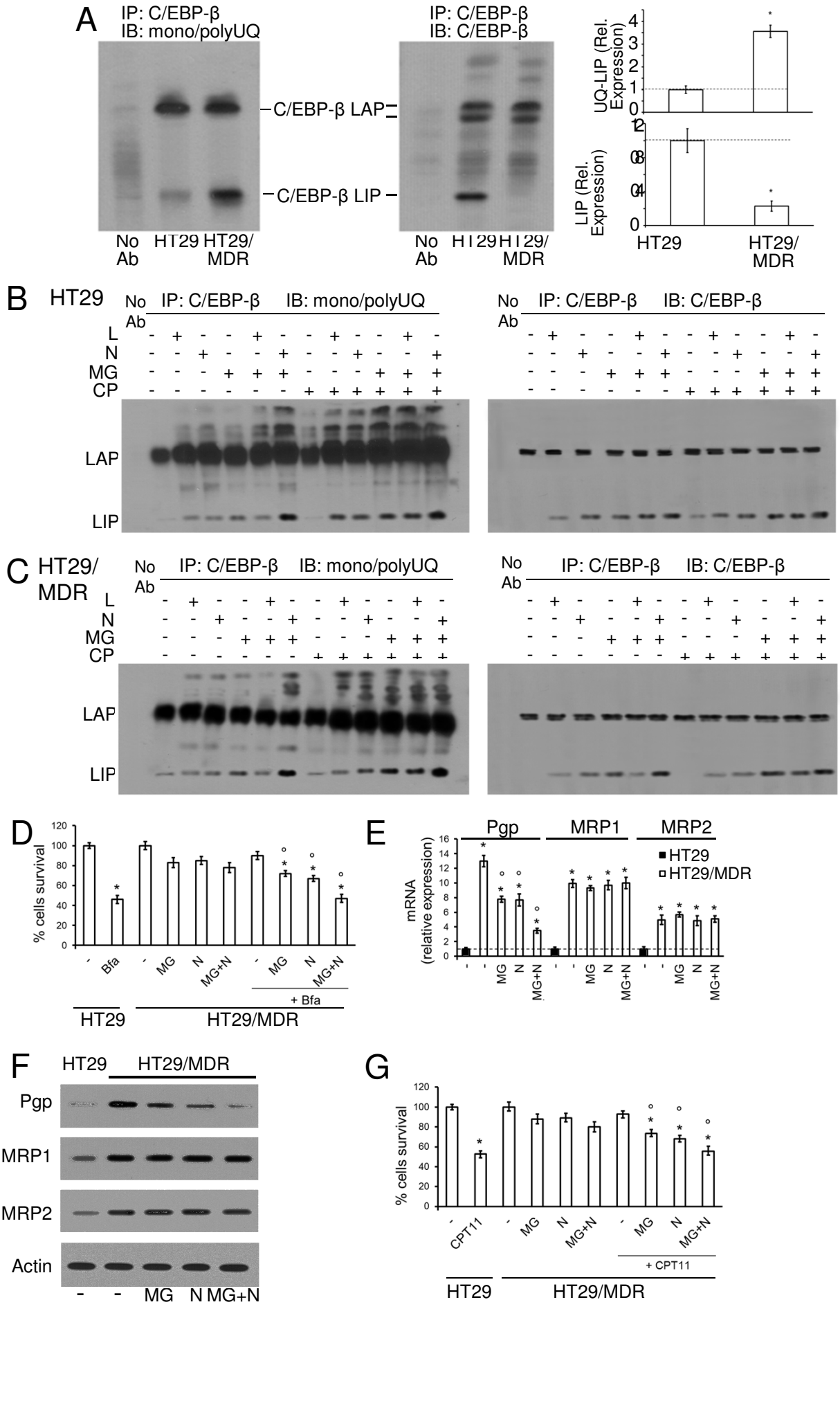
A
IP: C/EBP-β
IB: mono/polyUQ
C/EBP-β LAP
C/EBP-β LIP
No Ab
HT29
HT29/ MDR
IP: C/EBP-β
IB: C/EBP-β
UQ-LIP (Rel. Expression)
LIP (Rel. Expression)
B
HT29
L
N
MG
CP
LAP
LIP
C
HT29/ MDR
D
% cells survival
Bfa
MG
N
MG+N
+ Bfa
E
Pgp
MRP1
MRP2
mRNA (relative expression)
F
Pgp
MRP1
MRP2
Actin
G
CPT11
+ CPT11

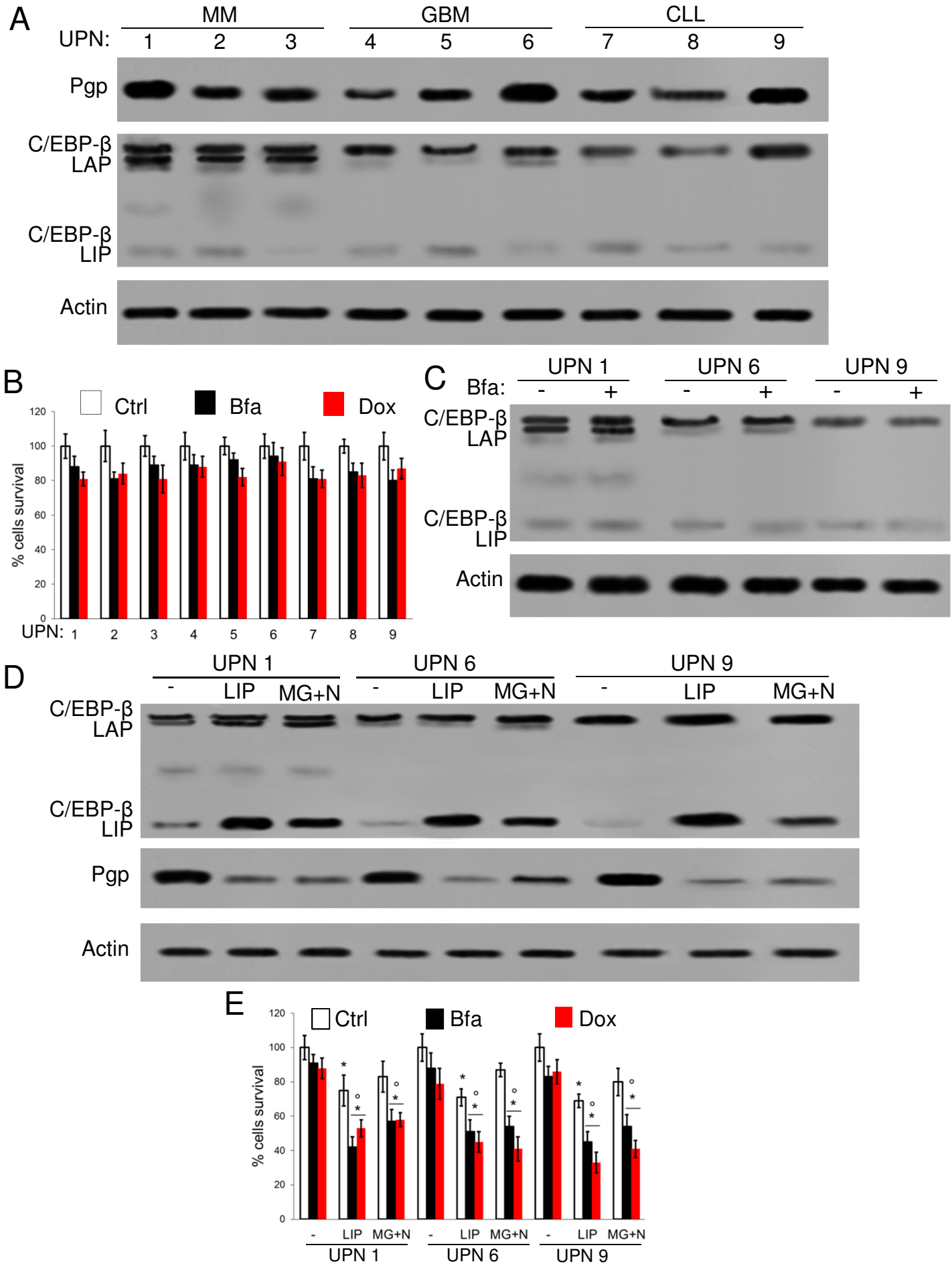
A
MM
GBM
CLL
UPN:
1
2
3
4
5
6
7
8
9
Pgp
C/EBP-β LAP
C/EBP-β LIP
Actin
B
Ctrl
Bfa
Dox
% cells survival
120
100
80
60
40
20
0
UPN:
1
2
3
4
5
6
7
8
9
C
Bfa:
UPN 1
UPN 6
UPN 9
-
+
-
+
-
+
C/EBP-β LAP
C/EBP-β LIP
Actin
D
UPN 1
UPN 6
UPN 9
-
LIP
MG+N
-
LIP
MG+N
-
LIP
MG+N
C/EBP-β LAP
C/EBP-β LIP
Pgp
Actin
E
Ctrl
Bfa
Dox
% cells survival
120
100
80
60
40
20
0
-
LIP
MG+N
-
LIP
MG+N
-
LIP
MG+N
UPN 1
UPN 6
UPN 9

Supplementary Materials

The Role of C/EBP-β LIP in Multidrug Resistance

Chiara Riganti[1], Joanna Kopecka[1], Elisa Panada[1], Sara Barak[2] and Menachem Rubinstein[2].

Supplementary Methods

Chemicals

Fetal bovine serum (FBS) and culture medium were purchased from Invitrogen Life Technologies (Carlsbad, CA). Plasticware for cell cultures was from Falcon (Becton Dickinson, Franklin Lakes, NJ). Irinotecan, 5-fluorouracil, oxaliplatin, cisplatin, doxorubicin, paclitaxel, thapsigargin, tunicamycin, and brefeldin A were from Sigma Chemical Co. (St. Louis, MO). Rhodamine 123 and MG132 were obtained from Merck Millipore (Billerica, MA). Electrophoresis reagents were from Bio-Rad Laboratories (Hercules, CA). The protein content of cell lysates was assessed with the BCA kit from Sigma. Unless otherwise indicated, all the other reagents were from Sigma.

Cell Lines

Human chemosensitive colon cancer HT29 cells and human chemosensitive non-small cell lung cancer A549 cells were from ATCC (Rockville, MD). The chemoresistant HT29/MDR and A549/MDR cell lines, used as models of acquired MDR (**Supplementary Table 1**), were generated by culturing parental cells in the presence of increasing concentrations of doxorubicin for 20 passages (20), and maintaining the cultures in media containing 250 nM doxorubicin (HT29/MDR) or 50 nM doxorubicin (A549/MDR). JC cells (ATCC) have been previously described as constitutively chemoresistant mammary cancer cells (21), syngeneic with the BALB/c mouse strain. Caco-2 cells (ATCC) are constitutively chemoresistant colon cancer cells (22). Samples of primary chemoresistant human pleural malignant mesothelioma were collected from the Biologic Bank of Malignant Mesothelioma, Santi Antonio e Biagio Hospital, Alessandria, Italy; samples of primary chemoresistant human glioblastoma multiforme were collected from the Neuro-Bio-Oncology Center, Vercelli, Italy; samples of primary chemoresistant chronic lymphocytic leukemia were collected from the Hematology Division, San Giovanni Battista Hospital, Torino, Italy. The samples were labelled with an “Unknown Patient Number” (UPN) in the

manuscript. The experimental protocol was approved by the Bioethics Committee ("Comitato Etico di Ateneo") of the University of Torino, Italy.

Generation of Drug Resistant Cells

HT29/MDR and A549/MDR cells were generated from parental HT29 and A549 cells by culturing cells in medium with increasing concentrations of doxorubicin up to 34 nM [1]. The resulting HT29/MDR cells were subjected to further selection with increasing concentrations of doxorubicin, up to 250 nM. This concentration of doxorubicin induced the expression of MRP1, MRP2, MRP5 and BCRP (**Supplementary Figure 1**) that were previously undetectable in the HT29/MDR clone [1]

Cell Viability and Growth

Counting of viable cells was performed as reported (18): 100,000 cells were seeded in 96-well plates and treated for 48 h as reported in the Results section, then stained with neutral red solution. The absorbance at 540 nm was read using a Packard EL340 microplate reader (Bio-Tek Instruments, Winooski, VT). The absorbance of untreated cells was considered as 100% viability; the results were expressed as percentage of viable cells vs. untreated cells. To evaluate morphology, cells were stained with 5% w/v crystal violet solution in 66% v/v methanol, washed and analyzed under bright field Olympus IX73 microscope (Olympus Corporation, Tokyo, Japan), equipped with the CellSense Dimension imaging system (10 x objective; 10 x ocular lens). To measure cell growth, HT29 or HT29/MDR cells (50,000/well), or JC cells (25,000/well) were seeded in 96-well plate, and after 8 h ("t_0") incubated with the indicated experimental stimuli for 12, 24, 48 or 72 h. The cultures were then stained with crystal violet as above and the absorbance was read at 570 nm. A titration curve obtained by reading crystal violet-stained serial dilutions of cells (i.e. 25,000, 50,000, 100,000, 200,000, 400,000, 800,000 cells) was established for each cell line, enabling conversion of the absorbance units into cell counts.

Over-Expression of LAP and LIP

The pcDNA4/TO expression vectors for C/EBP-β LAP and C/EBP-β LIP, produced as reported previously (18), were used to generate HT29 cells transiently over-expressing LAP and HT29/MDR cells transiently over-expressing LIP. Clones of HT29/MDR and JC cells stably and inducibly over-expressing LIP (HT29/MDR TetON LIP and JC TetON LIP) were generated by co-transducing pcDNA6/TR (Invitrogen Life Technologies, Milan, Italy) and pcDNA4/TO LIP plasmids in parental cells, then selecting cells with 2 μg/ml blasticidin S (Invitrogen Life Technologies) and 100 μg/ml zeocin (InvivoGen, San Diego, CA).

In Vivo Tumor Growth

1 x 10^5 JC TetON LIP cells in 20 µl culture medium mixed with 20 µl Cultrex BME (Trevigen, Gaithersburg, MD) were orthotopically implanted according to (23) in 6 weeks old female BALB/c mice, housed under 12 h light/dark cycle, with food and drinking provided ad libitum. Tumor growth was measured daily by caliper, and was calculated according to the equation $(LxW^2)/2$, where L = tumor length and W = tumor width. When tumor reached the volume of 100 mm^3, mice were randomized into four groups: "control" group (treated with 3 i.p. injections of saline, every 5 days), "doxycycline" group (treated as "control" group plus 1 mg/ml doxycycline in the drinking water), "doxorubicin" group (treated with 3 i.p. injections of 5 mg/kg doxorubicin, every 5 days), and "doxorubicin + doxycycline" group (treated as "doxorubicin" group plus 1 mg/ml doxycycline in the drinking water). Drinking water consumption was checked twice a day to monitor the complete doxycycline intake; drinking water with freshly prepared doxycycline was replaced at least every 2 days. Tumor volumes were monitored daily and animals were euthanized at day 15 after the first injection. Tumors were resected, photographed and fixed in 4% v/v paraformaldehyde. The paraffin sections were stained with hematoxylin/eosin or immunostained for Ki67, HERPUD1 or Pgp. The Institutional Animal Care and Use Committee of the Weizmann Institute of Science approved all animal protocols.

Immunoblotting

Cells were rinsed with PBS and then suspended in lysis buffer (50 mM Tris-HCl, 1 mM EDTA, 1 mM EGTA, 150 mM NaCl, 1% v/v Triton-X100; pH 7.4), supplemented with the protease inhibitor cocktail set III (80 µM aprotinin, 5 mM bestatin, 1.5 mM leupeptin, 1 mM pepstatin; Merck Millipore), 2 mM phenylmethanesulfonyl fluoride and 1 mM Na_3VO_4, then sonicated and the extract was clarified (13,000 x g, 10 min. at 4°C). Protein extracts (20 µg) were subjected to SDS-PAGE and probed with the following antibodies: ATF6, PERK, MRP1/ABCC1, MRP4/ABCC4 and MRP2/ABCC2 (Abcam, Cambridge, UK), IRE1α and phospho(Ser724)IRE1α (Thermo Scientific Inc., Rockford, IL), phospho(Thr980)PERK, eIF2α and phospho(Ser51)eIF2α (Cell Signaling Technology Inc., Danvers, MA), MRP3/ABCC3, MRP5/ABCC5, BCRP/ABCG2, C/EBP-β (C-19) and CHOP/GADD153 (Santa Cruz Biotechnology Inc., Santa Cruz, CA), caspase-3 (C33, GeneTex, Hsinhu City, Taiwan), TRB3 and HERPUD1 (Proteintech, Chicago, IL), Pgp/ABCB1 (C219, Novus Biologicals, Cambridge, UK), actin (Sigma Chemical Co.). Blotting was followed by the peroxidase-conjugated secondary anti-mouse or anti-rabbit antibody (Bio-Rad). The

membranes were washed with Tris-buffered saline (TBS)/Tween 0.01% v/v and proteins were detected by enhanced chemiluminescence (Bio-Rad Laboratories). To detect ubiquitinated C/EBP-β, 100 µg protein extracts were immuno-precipitated overnight with the anti-C/EBP-β antibody, using 25 µl of PureProteome Magnetic Beads (Merck Millipore). The immuno-precipitated samples were then resolved by SDS-PAGE and probed with an anti-mono/polyubiquitin antibody (FK2, Axxora, Lausanne, Switzerland). Densitometric analysis was performed using the ImageJ program.

PCR

Total RNA was extracted and reverse-transcribed using the QuantiTect Reverse Transcription Kit (Qiagen, Hilden, Germany). RT-PCR was carried out with IQ^{TM} SYBR Green Supermix (Bio-Rad Laboratories). The same cDNA preparation was used for the quantitation of *Pgp*, *MRP1*, *MRP2* and *actin*, chosen as housekeeping gene. The primers sequences were: *Pgp*: 5'-TGCTGGAGCGGTTCTACG-3'; 5'-ATAGGCAATGTTCTCAGCAATG-3'; *MRP1*: 5'-CATTCAGCTCGTCTTGTCCTG-3'; 5'-GGATTAGGGTCGTGGATGGTT-3'; *MRP2*: 5'-TGCTTCCTGGGGATAATCAG-3'; 5'-CAGGGATAACTGCAAACCT-3'; *actin*: 5'-GCTATCCAGGCTGTGCTATC-3'; 5'-TGTCACGCACGATTTCC-3'. The relative quantitation of each sample was performed using the Gene Expression Quantitation software (Bio-Rad Laboratories). For semi-quantitative PCR, cDNA was amplified with AmpliTaq Gold DNA Polymerase (Applied Biosystems, Carlsbad, CA). The primers sequences were: *C/EBP-β*: 5'-GACAAGCACAGCGACGACTA-3'; 5'-AGCTGCTCCACCTTCTTCTG-3'; *actin*: 5'-GGACTTCGAGCAAGAGATGG-3'; 5'-AGCACTGTGTTGGCGTACAG-3'. PCR products were visualized on 3% w/v agarose gel stained with 0.01% v/v ethidium bromide. PCR arrays were performed on 1 µg cDNA, using the Unfolded Protein Response Plus PCR Array (Qiagen), following the manufacturer's instructions. Data were analysed with the RT² Profiler™ PCR Array Data Analysis software (Qiagen).

Rhodamine 123 efflux

The efflux of rhodamine 123 was used to measure the Pgp activity [2]. Cells were washed with PBS, detached with Cell Dissociation Solution (Sigma Chemical Co.) and re-suspended at 5 x 10^5 cells/ml in 1 ml of culture medium. Samples were maintained at 37°C for 20 minutes in the presence of 1 µg/ml rhodamine 123. After this incubation time, cells were washed and re-suspended in 0.5 ml of PBS; the intracellular rhodamine content, which is inversely related to its efflux, was detected using a FACSCalibur system (Becton

Dickinson). For each analysis 100,000 events were collected. Data were analyzed by CellQuest software (Becton Dickinson).

Intracellular doxorubicin accumulation

For flow cytometer analysis, cells were washed with PBS, detached with Cell Dissociation Solution and re-suspended at 5 x 10^5 cells/ml in 1 ml of culture medium, then incubated 20 minutes at 37°C with 5 μM doxorubicin. After this incubation time, cells were washed and re-suspended in 0.5 ml of PBS; the intracellular content of doxorubicin was analyzed by FACSCalibur system, as reported above. For fluorescence microscopy, 0.1 x 10^5 JC cells were seeded in sterile chamber slides and incubated for 3 h with 5 μM doxorubicin. Cells were washed 3x with PBS, fixed in 4% v/v paraformaldehyde, washed 3x with PBS and counterstained with Hoechst 33258 (0.1 mg/ml, diluted 1: 5,000). Samples were analyzed using an Olympus IX73 microscope equipped with the CellSense Dimension imaging system (Olympus), using a 60 x objective (1.4 numerical aperture) and a 10 x ocular lens. For each experimental point, a minimum of 5 microscopic fields were examined.

Cell cycle analysis

Cells were washed twice with fresh PBS, incubated in 0.5 ml ice-cold 70% v/v ethanol for 15 min, then centrifuged at 1,200 x g for 5 min at 4°C and rinsed with 0.3 ml of citrate buffer (50 mM Na_2HPO_4, 25 mM sodium citrate, 10 v/v % Triton X-100), containing 10 μg/ml propidium iodide and 1 mg/ml RNAse (from bovine pancreas). After 15 min incubation in the dark, the intracellular fluorescence was detected by a FACSCalibur flow cytometer (Becton Dickinson). For each analysis, 10,000 events were collected and analyzed by the Cell Quest software (Becton Dickinson).

Supplementary References

[1]. Riganti C, Miraglia E, Viarisio D*, et al.* Nitric oxide reverts the resistance to doxorubicin in human colon cancer cells by inhibiting the drug efflux. *Cancer Res.* 2005;65(2):516-525.

[2]. Sarkadi B, Homolya L, Szakacs G, Varadi A. Human multidrug resistance ABCB and ABCG transporters: Participation in a chemoimmunity defense system. *Physiol Rev* 2006;86(4):1179-1236.

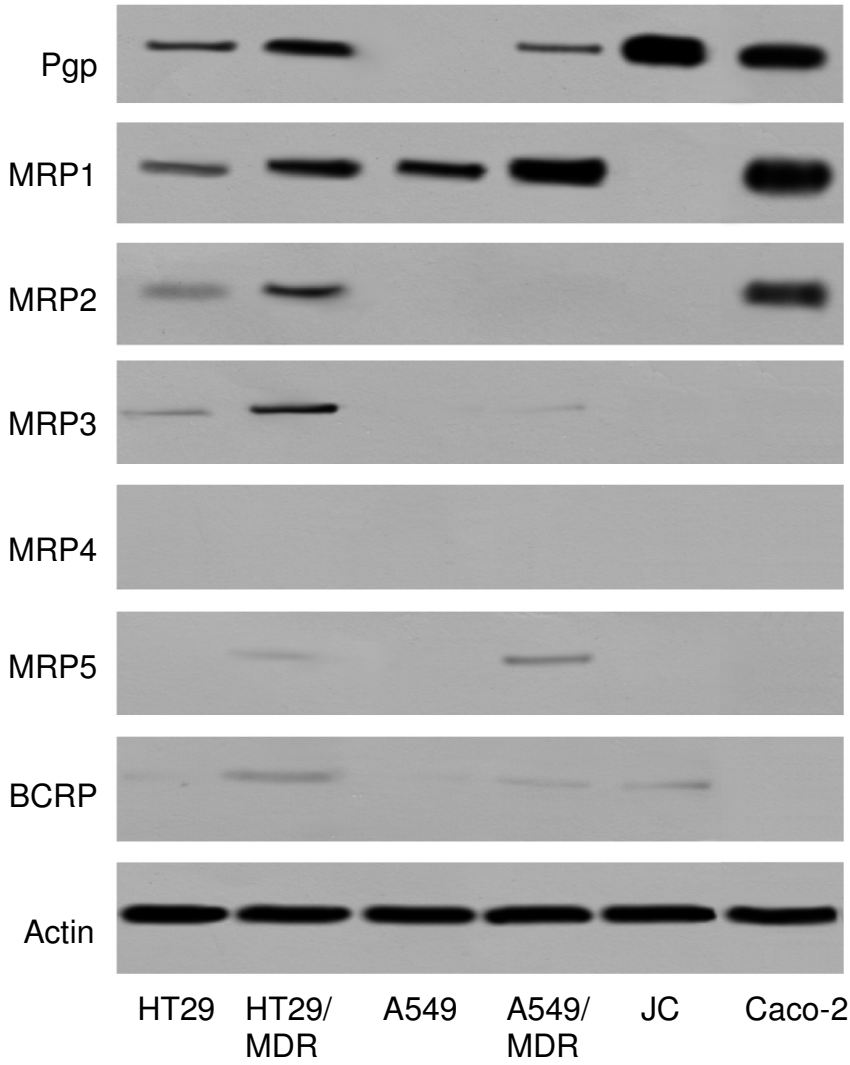

Supplementary Figure 1. Expression of ABC Transporters in Chemosensitive and Chemoresistant Cells. Extracts from human chemosensitive colon cancer HT29 cells and chemoresistant HT29/MDR cells, human chemosensitive non small cell lung cancer A549 cells and chemoresistant A549/MDR cells, mouse chemoresistant mammary cancer JC cells and human chemoresistant colon cancer Caco-2 cells were resolved by SDS-PAGE and immunoblotted with the indicated antibodies. An anti-actin antibody was used as a load control.

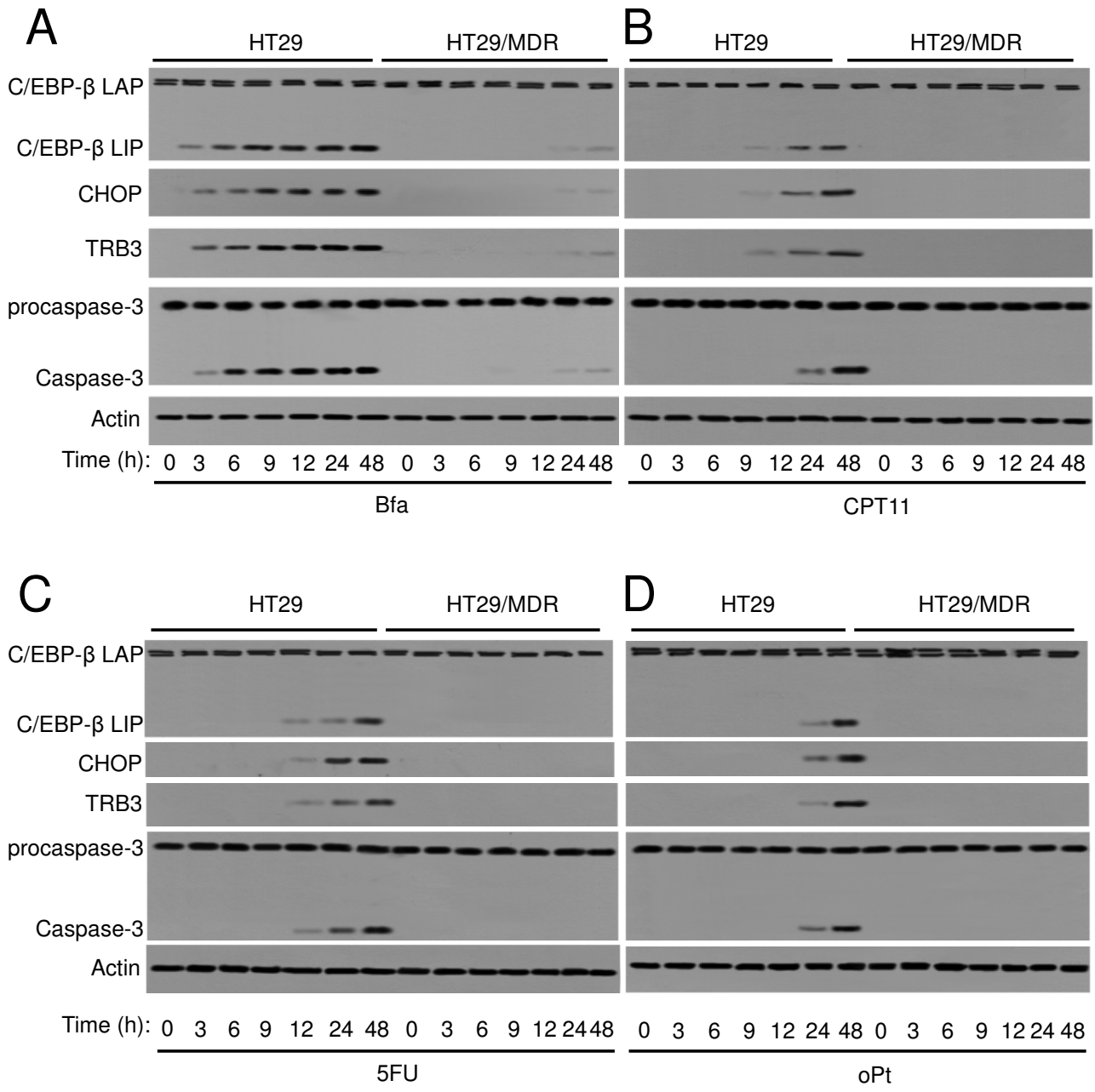

Supplementary Figure 2. Kinetics of expression of C/EBP-β LIP, CHOP, TRB3, and Caspase-3 in Chemosensitive and Chemoresistant Cells. HT29 and HT29/MDR were incubated in media without (0) or with brefeldin A (50 nM, Bfa; panel **A**), irinotecan (10 μM, CPT11; panel **B**), 5-fluorouracil (5 μM, 5FU; panel **C**), oxaliplatin (5 μM, oPt; panel **D**) for the indicated times. Cell extracts were resolved by SDS-PAGE and immunoblotted with the indicated antibodies. Anti C/EBP-β recognizes both LAP and LIP; anti caspase-3 recognizes both procaspase-3 and cleaved caspase-3. Actin served as a load control.

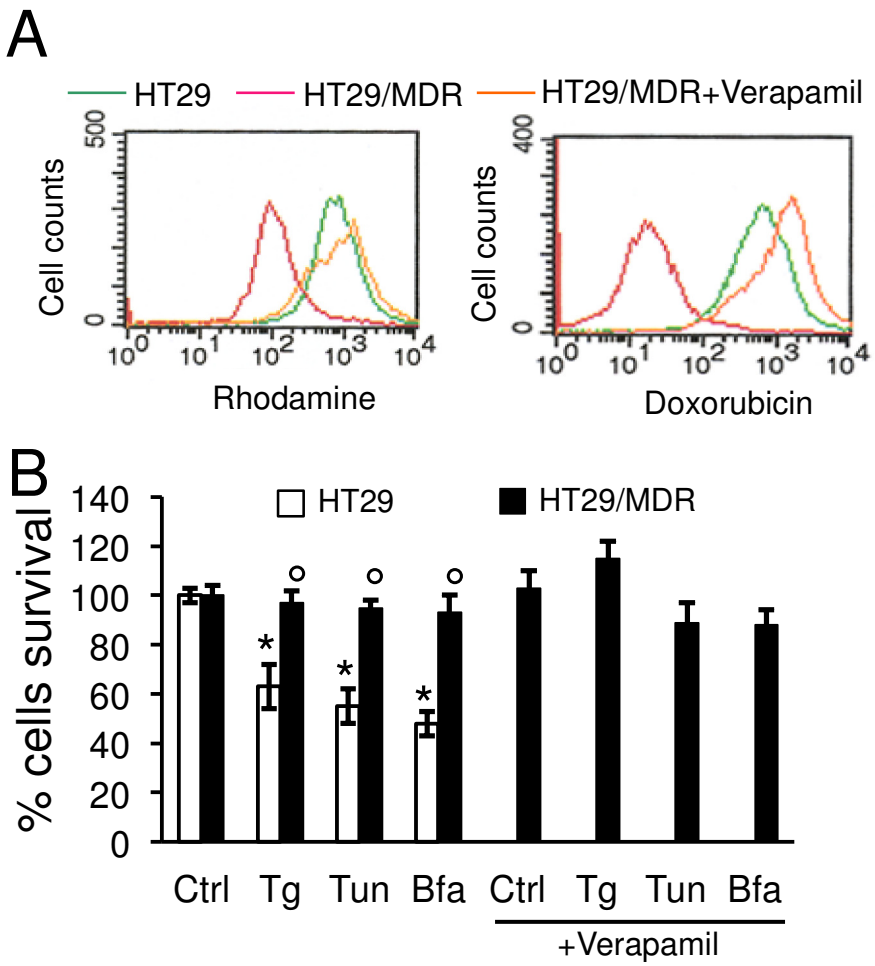

Supplementary Figure 3. The Role of Pgp in the Cellular Response to ER Stress. A) HT29 cells were incubated for 20 minutes at 37°C with the Pgp substrates rhodamine 123 (1 µg/mL, left panel) or doxorubicin (5 µM, right panel). HT29/MDR were pre-incubated with medium or with the Pgp inhibitor verapamil (10 mM) for 1 h followed by incubation for 20 minutes at 37°C with the Pgp substrates rhodamine 123 (1 µg/mL, left panel) or doxorubicin (5 µM, right panel). The intracellular content of rhodamine 123 or doxorubicin, taken as index of Pgp activity, was measured by flow cytometry. **B**) Cells were grown for 48 h in media without (Ctrl) or with thapsigargin (50 nM, Tg), tunicamycin (1 µM, Tun) or brefeldin A (50 nM, Bfa), alone or together with verapamil (10 mM). Cell viability was assessed in quadruplicate by neutral red staining. Data are presented as means±SD (n=4). **P*=0.01, 0.007, and 0.005 for thapsigargin (Tg)-, tunicamycin (Tun)-, and brefeldin A (Bfa)-treated HT29 cells, respectively, vs. untreated (Ctrl) HT29 cells; °*P*=0.02, 0.008, and 0.006 for Tg-, Tun-, and Bfa-treated HT29/MDR cells, respectively, vs. drug-treated HT29 cells (two-sided ANOVA).

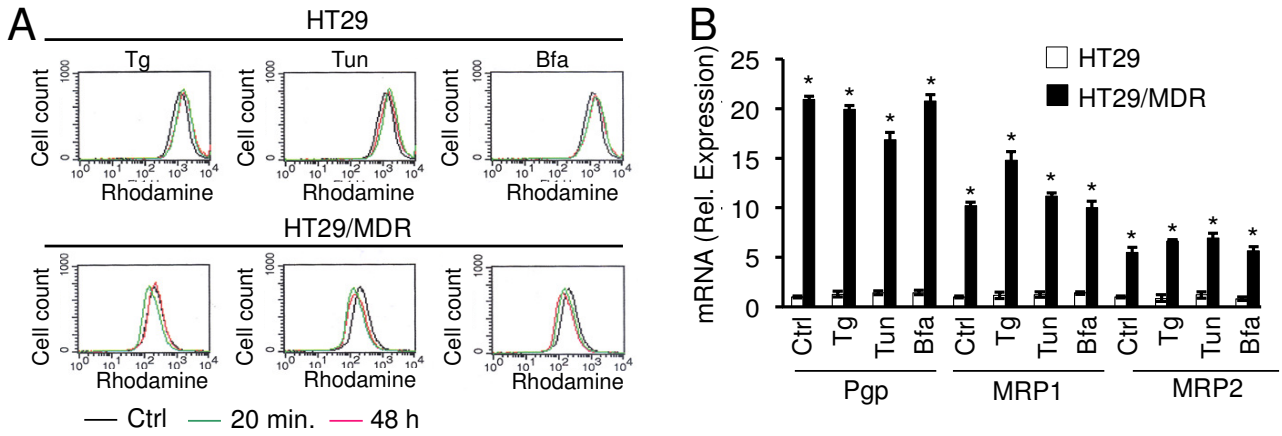

Supplementary Figure 4. The Impact of ER Stress on ABC Transporter's Activity and Gene Expression. A) HT29 and HT29/MDR cells were incubated for 20 minutes at 37°C with the Pgp substrate rhodamine 123 (1 µg/mL) in the absence (Ctrl) or presence of thapsigargin (50 nM), tunicamycin (1 µM), brefeldin A (50 nM) (Tg/Tun/Bfa 20 min). In parallel, cells were pre-treated for 48 h with the same concentrations of thapsigargin, tunicamycin or brefeldin A (Tg/Tun/Bfa 48 h) and then incubated with rhodamine 123. The intracellular content of rhodamine 123, taken as index of Pgp activity, was measured by flow cytometry. **B**) HT29 and HT29/MDR cells were grown for 24 h in media without (Ctrl) or with thapsigargin (50 nM, Tg), tunicamycin (1 µM, Tun) or brefeldin A (50 nM, Bfa), then total RNA was extracted, reverse-transcribed and subjected to qRT-PCR for *Pgp, MRP1, and MRP2* mRNA. Measurements were performed in triplicate and data are presented as means±SD (n=3). For all three transporters **P*<0.001 for HT29 vs. HT29/MDR cells (two-sided ANOVA).

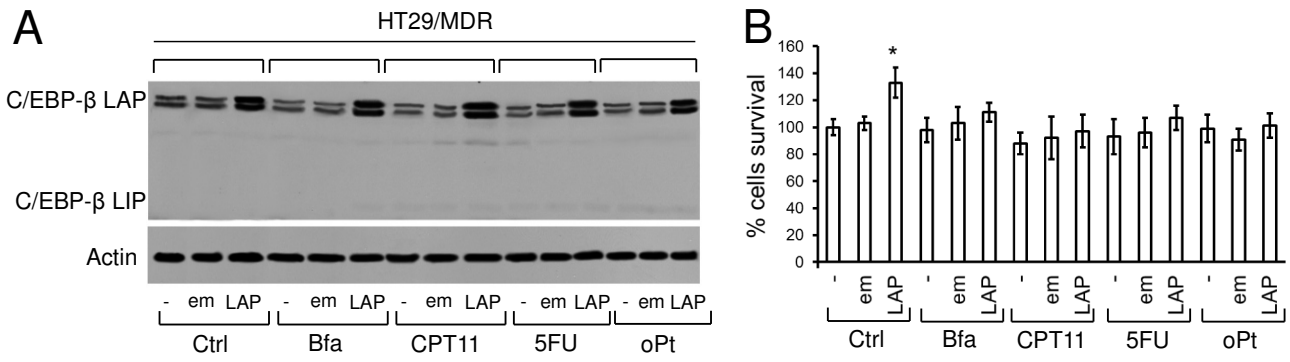

Supplementary Figure 5. The Impact of C/EBP-β LAP Over-Expression on Cell Viability Upon ER Stress and Chemotherapy. Control HT29/MDR cells (-), cells transfected with empty pcDNA4/TO vector (em) or with pcDNA4/TO expression vector encoding C/EBP-β LAP(LAP), were grown for 48 h in media without or with brefeldin A (Bfa, 50 nM), irinotecan (CPT11,10 μM), 5-fluorouracil (5FU, 5 μM) or oxaliplatin (oPt, 5 μM). **A**) Cell extracts were resolved by SDS-PAGE and immunoblotted with antibody recognizing the common C-terminal peptide of C/EBPβ LAP and LIP. Blotting with anti-actin antibody served as a load control. **B**) Cell viability following treatments with vehicle or the indicated agents as in A. Viability was assessed in quadruplicate by neutral red staining. Data are presented as means±SD (n=4). *P=0.04 for the LAP-expressing cells vs. un-transfected cells (two-sided ANOVA).

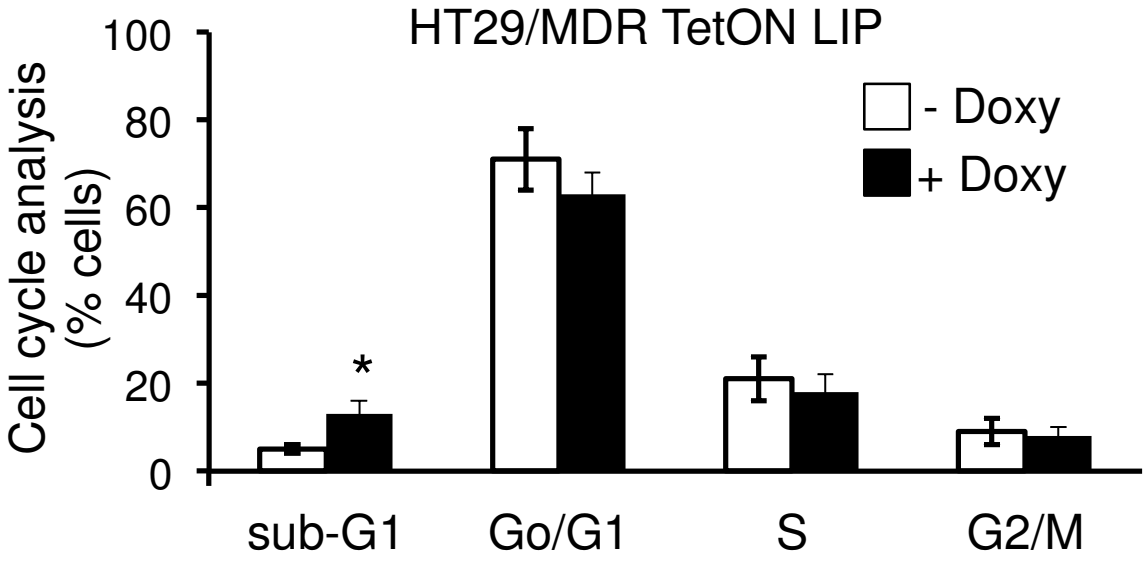

Supplementary Figure 6. Effects of C/EBP-β LIP on Cell Cycle Progression.
HT29/MDR TetON LIP cells, stably transfected with the inducible pcDNA4/TO expression vector encoding C/EBPβ LIP, were cultured for 48 h in media without (- Doxy) or with 1 μg/ml doxycycline (+ Doxy). The cells distribution in sub-G1, G0/G1, S, and G2/M phases was analyzed by flow cytometry. Data are presented as means±SD (n=4). *P=0.04 (two-sided ANOVA).

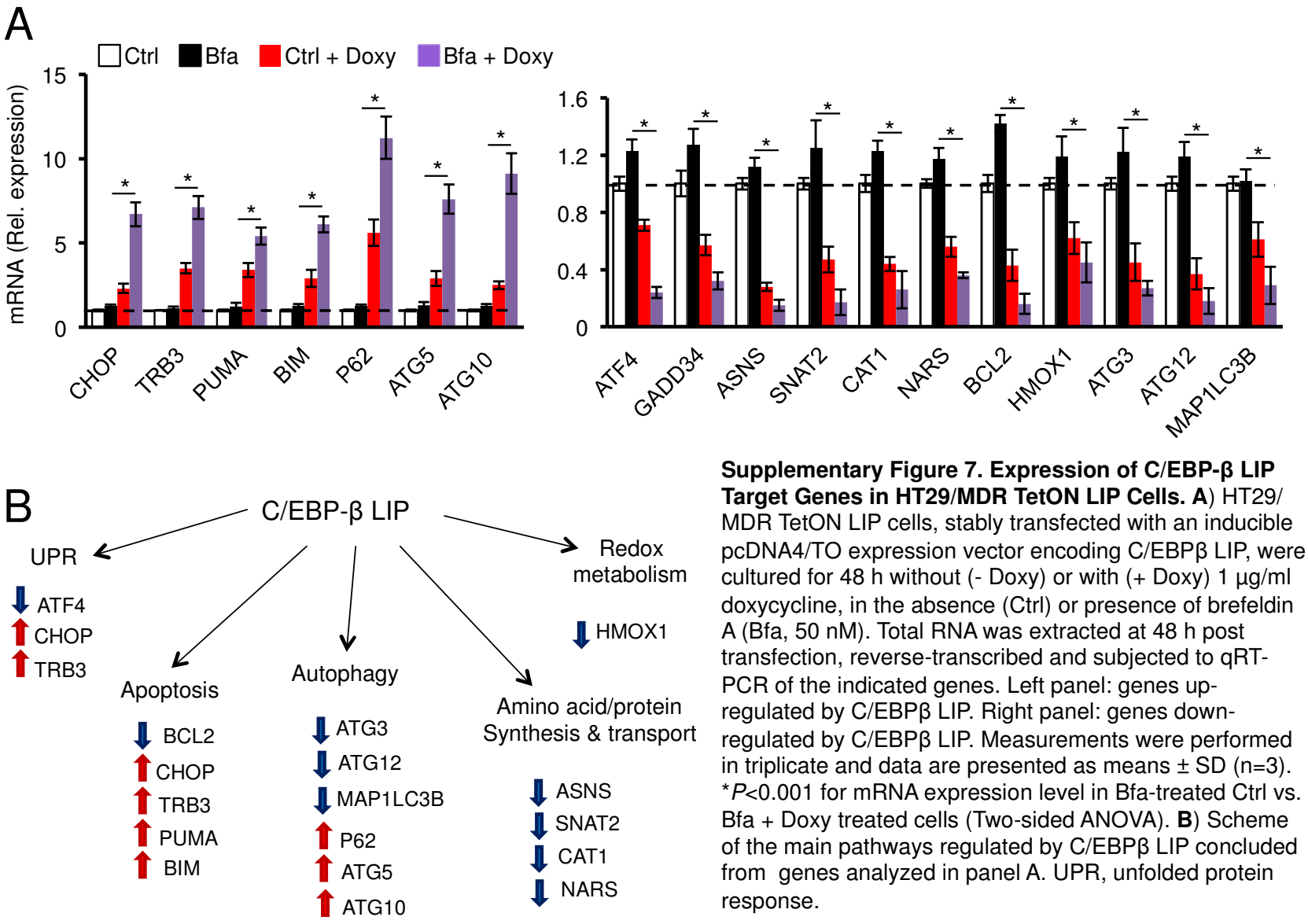

Supplementary Figure 7. Expression of C/EBP-β LIP Target Genes in HT29/MDR TetON LIP Cells. A) HT29/MDR TetON LIP cells, stably transfected with an inducible pcDNA4/TO expression vector encoding C/EBPβ LIP, were cultured for 48 h without (- Doxy) or with (+ Doxy) 1 µg/ml doxycycline, in the absence (Ctrl) or presence of brefeldin A (Bfa, 50 nM). Total RNA was extracted at 48 h post transfection, reverse-transcribed and subjected to qRT-PCR of the indicated genes. Left panel: genes up-regulated by C/EBPβ LIP. Right panel: genes down-regulated by C/EBPβ LIP. Measurements were performed in triplicate and data are presented as means ± SD (n=3). *P<0.001 for mRNA expression level in Bfa-treated Ctrl vs. Bfa + Doxy treated cells (Two-sided ANOVA). **B**) Scheme of the main pathways regulated by C/EBPβ LIP concluded from genes analyzed in panel A. UPR, unfolded protein response.

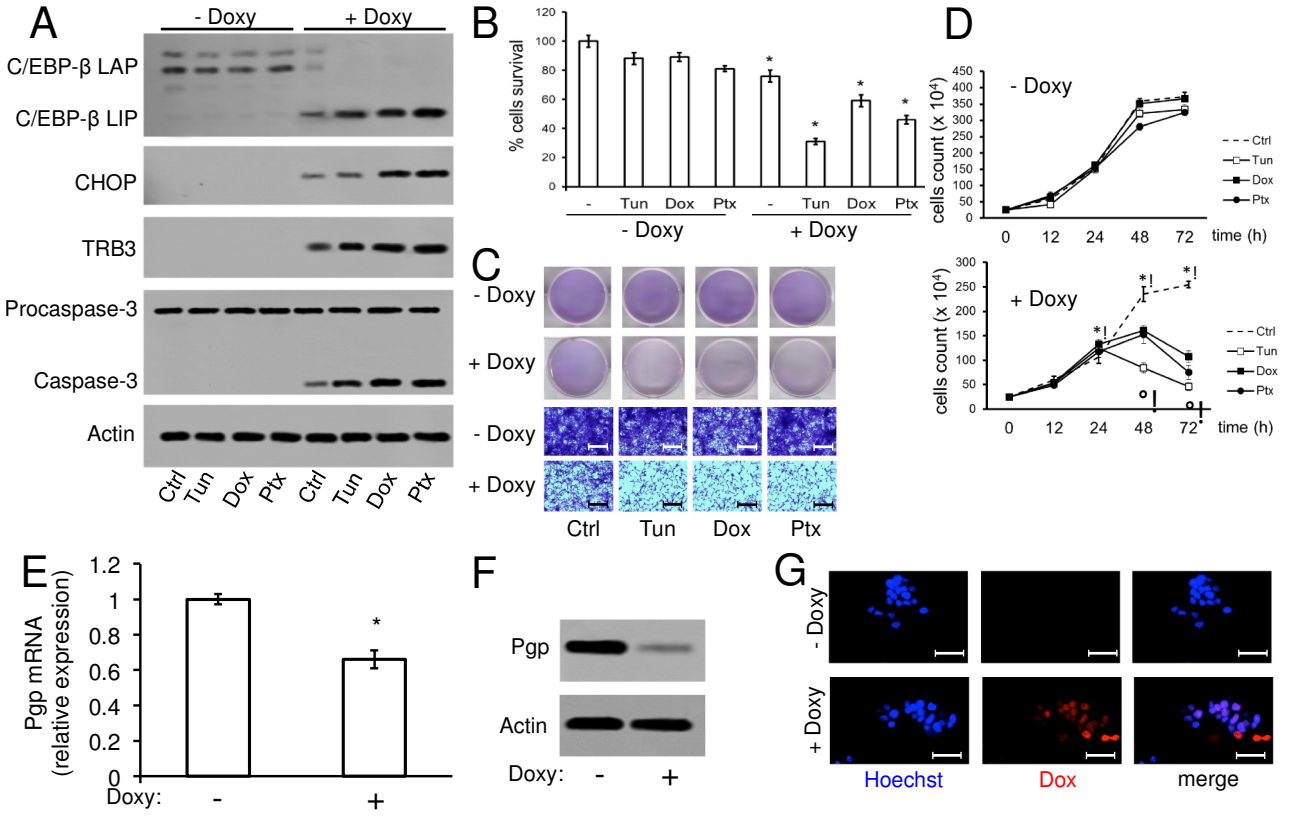

Supplementary Figure 8. The Impact of C/EBP-β LIP Induction on Resistance of JC Cells to ER Stress- and Chemotherapy and on Pgp Expression. JC TetON LIP cells, stably transfected with the inducible pcDNA4/TO expression vector for C/EBP-β LIP, were cultured for 24 h in media without (-Doxy) or with 1 μg/ml doxycycline (+Doxy), in the absence (Ctrl) or presence of tunicamycin (1 μM, Tun), doxorubicin (5 μM, Dox) or paclitaxel (10 μM, Ptx). **A**) Cell extracts were resolved by SDS-PAGE and immunoblotted with the indicated antibodies. Anti C/EBP-β recognizes both LAP and LIP; anti caspase-3 recognizes both procaspase-3 and cleaved caspase-3. Actin served as a load control. **B**) Cells (10^5/well) were cultured for 24 h in 96-well plates as in A, cell viability was then assessed in quadruplicate by neutral red staining. Data are presented as means±SD (n=3). *P=0.04, 0.002, 0.01, and 0.009 for "+Doxy", "+Doxy+Tun", "+Doxy+Dox" and "+Doxy+Ptx", respectively, vs. "-Doxy" cells (two-sided ANOVA). **C**) Cells (10^5/well) were grown for 24 h in 96-well plates as in A and then stained with crystal violet and photographed (upper panels, 1x; lower panels, bright field microscopy). For each experimental point, a minimum of 5 microscopic fields were examined. Bars = 500 μM. **D**) Cells (25,000/well) were cultured in 96-well plates without (Ctrl) or with tunicamycin, doxorubicin, or paclitaxel as in A. The cell number was determined in quadruplicates following fixation and crystal violet staining at the indicated times. Data are presented as mean±SD (n=4). * P=0.04 (24 h), * P=0.006 (48 h), * P=0.005 (72 h), for untreated (Ctrl)

"+Doxy" cells vs. untreated (Ctrl) "-Doxy" cells; °P<0.001 for cells treated with tunicamycin (Tun), doxorubicin (Dox) or paclitaxel (Ptx), vs. untreated cells at 72 h (two-sided ANOVA). **E**) Total RNA was extracted from JC TetON LIP cells grown in the absence (-) or presence (+) of doxycycline, reverse-transcribed and subjected to qRT-PCR for *Pgp* mRNA. Measurements were performed in triplicate and data are presented as means±SD (n=3). * P=0.04 for "+Doxy" cells vs. "-Doxy" cells (two-sided ANOVA). **F**) Cell extracts of JC TetON LIP cells, grown in the absence (-) or presence (+) of doxycycline for 48 h, were resolved by SDS-PAGE and immunoblotted with anti Pgp antibody. Actin served as a load control. **G**) JC TetON LIP cells, grown for 48 h in the absence (-) or presence (+) of doxycycline (Doxy), were incubated for 3 h with doxorubicin (5 µM, Dox), counterstained with Hoechst 33258 and analyzed by fluorescence microscopy. Bars = 20 µM.